"CORRELATION OF PERIPAPILLARY RETINAL NERVE FIBRE LAYER THICKNESS AND MACULAR GANGLION CELL LAYER- INNER PLEXIFORM LAYER THICKNESS WITH VISUAL FIELD CHANGES IN PATIENTS OF PRIMARY OPEN ANGLE GLAUCOMA BY SPECTRAL DOMAIN OPTICAL COHERENCE TOMOGRAPHY."

BY

REG NO: BK0122003

Dissertation

Submitted to the KLE Academy of Higher Education and Research, Belagavi, Karnataka

In Partial Fulfilment

of the Requirements for the Degree of

MASTER OF SURGERY

IN

OPHTHALMOLOGY

DEPARTMENT OF OPHTHALMOLOGY
JAWAHARLAL NEHRU MEDICAL COLLEGE,
BELAGAVI, KARNATAKA

SEPTEMBER /OCTOBER 2025

KLE ACADEMY OF HIGHER EDUCATION AND RESEARCH,

BELAGAVI, KARNATAKA.

Endorsement

This is to certify that the dissertation entitled **"CORRELATION OF PERIPAPILLARY RETINAL NERVE FIBRE LAYER THICKNESS AND MACULAR GANGLION CELL LAYER- INNER PLEXIFORM LAYER THICKNESS WITH VISUAL FIELD CHANGES IN PATIENTS OF PRIMARY OPEN ANGLE GLAUCOMA BY SPECTRAL DOMAIN OPTICAL COHERENCE TOMOGRAPHY"** is a bonafide research work done by **(REG NO: BK0122003).**

Dr. SHIVANAND C BUBANALE
MS (Ophthalmology) F.I.G.O
Professor and Head
Department of Ophthalmology
J. N. Medical College,
Nehru Nagar, Belagavi – 590010

Date: 22/03/2025
Place: JNMC, Belagavi

Dr. N S MAHANTASHETTI M.D.
Principal
J.N. Medical College,
Nehru Nagar, Belagavi - 590010

PRINCIPAL
Jawaharlal Nehru Medical College
BELAGAVI

Date: 22/03/2025
Place: JNMC, Belagavi

UNDERTAKING

I, **(REG NO: BK0122003)**, hereby declare that the information and data mentioned in my dissertation entitled **"CORRELATION OF PERIPAPILLARY RETINAL NERVE FIBRE LAYER THICKNESS AND MACULAR GANGLION CELL LAYER- INNER PLEXIFORM LAYER THICKNESS WITH VISUAL FIELD CHANGES IN PATIENTS OF PRIMARY OPEN ANGLE GLAUCOMA BY SPECTRAL DOMAIN OPTICAL COHERENCE TOMOGRAPHY"** belongs to me and is original. I am aware of the definition of plagiarism as detailed below:

- An act or instance of using or closely imitating the language and thoughts of another author without authorization and the representation of that author's work as one's own, as by not crediting the original author.
- A piece of writing or other work reflecting such unauthorized use or imitation.
- The deliberate or reckless representation of another's words, thoughts or ideas as one's own without attribution in connection with submission of academic work whether graded or otherwise.

I hereby declare that the dissertation prepared by me is original one and does not involve plagiarism anywhere. In case at a later stage, it is found that I have indulged in plagiarism, then I am solely responsible for the same and the institution is at liberty to take any disciplinary action against me including cancellation of dissertation or any other penalties imposed by the University.

Date:17-03-2025

Place: JNMC, Belagavi **(REG NO: BK0122003)**

PLAGIRISM CLERANCE

KLE JAWAHARLAL NEHRU MEDICAL COLLEGE
(A constituent unit of KLE Academy of Higher Education & Research Deemed-to-be-University)
(Recognized by National Medical Commission, New Delhi)
Accredited 'A+' Grade by NAAC (3rd Cycle) Placed in Category 'A' by MoE (GoI)
Nehru Nagar, Belagavi- 590 010, Karnataka, INDIA
0831 - 2471350 0831 - 2470759 www.jnmc.edu incipal@jnmc.edu

Ref No: MDC/PG/ Date: 19-03-2025

"ACCEPTANCE LETTER"

The softcopy of thesis entitled: **"CORRELATION OF PERIPAPILLARY RETINAL NERVE FIBRE LAYER THICKNESS AND MACULAR GANGLION CELL LAYER-INNER PLEXIFORM LAYER THICKNESS WITH VISUAL FIELD CHANGES IN PATIENTS OF PRIMARY OPEN ANGLE GLAUCOMA BY SPECTRAL DOMAIN OPTICAL COHERENCE TOMOGRAPHY"** has been submitted for anti-plagiarism check through Turnitin software. The scan has been carried out and the scanned output reveals a match percentage of **10%** which is within the acceptable limits of **10%** as per the guidelines given by UGC.

Jyothisri
Guide.

KAHER BELAGAVI J.N. MEDICAL COLLEGE

Dr. (Mrs.) N.S. Mahantashetti.
Chairperson-Antiplagiarism Committee &
Principal,
J. N. Medical College, Belagavi.

To,
Reg. No. BK0122003
Postgraduate Student,
2022-23 Batch,
Department of Ophthalmology
J. N. Medical College, Belagavi.

ETHICAL CLERANCE

K.L.E. ACADEMY OF HIGHER EDUCATION AND RESEARCH
(Deemed – to- be- University)
Accredited 'A+' Grade by NAAC in (3rd Cycle) Placed in Category 'A' by MHRD (GoI)
JNMC INSTITUTIONAL ETHICS COMMITTEE
JAWAHARLAL NEHRU MEDICAL COLLEGE,
NEHRU NAGAR, BELAGAVI-590010 (KARNATAKA-INDIA)
Website: http//www.jnmc.edu
E-Mail : dome@jnmc.edu
Phone: (+ 91-(0)831 Office : 2472550
Principal: 2471701
Fax No. +91 (0)831 – 2470759

Ref No.MDC/JNMCIEC/ 176 **Date: 21/04/2023**

To,

(REG NO: BK0122003)
PG Student in Ophthalmology
J. N. Medical College,
BELAGAVI.

Sub: Institutional Ethical Clearance for the study.

With reference to the above, we wish to inform you that your proposed research project titled **"CORRELATION OF PERIPAPILLARY RETINAL NERVE FIBER LAYER THICKNESS AND MACULAR GANGLION CELL LAYER- INNER PLEXIFORM LAYER THICKNESS WITH VISUAL FIELD CHANGES IN PATIENTS OF PRIMARY OPEN ANGEL GLAUCOMA BY SPECTRAL DOMAIN OPTICAL COHERENCE TOMOGRAPHY",** is ethical and justifiable. The proposed research project has been cleared by the JNMC Institutional Ethics Committee.

(Dr. Smita Sonoli)
Member Secretary
JNMC Institutional Ethics Committee
J.N.Medical College, Belagavi.

(Dr. Harsha Hegde)
Chairman,
JNMC Institutional Ethics Committee
J.N.Medical College, Belagavi

LIST OF ABBREVIATIONS

POAG	Primary open angle glaucoma
AT	Applanation tonometry
BCVA	Best-corrected visual acuity
BMO-MRW	Bruch's membrane opening minimum rim width
cpRNFL	Circumpapillary retinal nerve fiber layer
CRA	Central retinal artery
FD-OCT	Fourier domain optical coherence tomography
GCC	Ganglion cell complex
GC-IPL	Ganglion cell-inner plexiform layer
GCL	Ganglion cell layer
HVF	Humphery visual field
IOP	Intraocular pressure
LC	Lamina cribrosa
MD	Mean deviation

OCT	Optical coherence tomography
OCTA	Optical coherence tomography angiography
ONH	Optic nerve
POAG	Primary open angle glaucoma
PSD	Pattern standard deviation
RAPD	Relative afferent pupillary defect
RGCs	Retinal ganglion cells
RNFL	Retinal nerve fibre layer
SD-OCT	Spectral domain optical coherence tomography
SS-OCT	Swept source optical coherence tomography
TD-OCT	Time domain optical coherence tomography
VF	Visual field

ABSTRACT

Introduction

Primary open-angle glaucoma (POAG) is a chronic optic neuropathy leading to progressive retinal ganglion cell (RGC) loss, retinal nerve fiber layer (RNFL) thinning, and visual field (VF) defects. Early detection and disease monitoring are critical in preventing irreversible blindness. Spectral-domain optical coherence tomography (SD-OCT) has emerged as a valuable imaging tool for assessing peripapillary RNFL and macular ganglion cell layer-inner plexiform layer (GC-IPL) thickness. This study aims to evaluate structural damage in POAG patients using SD-OCT and correlate these findings with visual field changes determined by Humphrey Visual Field (HVF) analysis.

Methodology

A hospital-based observational cross-sectional study was conducted over one year, including 34 POAG patients. Inclusion criteria encompassed adults diagnosed with POAG, while those with significant ocular comorbidities were excluded. Peripapillary RNFL and GC-IPL thicknesses were measured using SD-OCT, and VF analysis was performed using the HVF 30-2 SITA Standard. Statistical analysis included correlation assessments between structural and functional parameters, using SPSS software.

Results

The study revealed significant thinning of RNFL and GC-IPL layers with increasing glaucoma severity. Mean deviation (MD) and pattern standard deviation (PSD) values

progressively worsened from early to advanced glaucoma. A strong correlation was found between MD and RNFL thinning in advanced glaucoma (p=0.003), whereas GC-IPL thinning demonstrated a significant association with MD across all stages (p=0.017). These findings highlight the increasing structural-functional relationship as glaucoma progresses.

Conclusion

RNFL and GC-IPL thickness assessments provide crucial insights into glaucoma progression. GC-IPL thickness exhibited a stronger correlation with visual field defects, making it a valuable parameter for early glaucoma detection. Combining SD-OCT with VF analysis enhances diagnostic accuracy and facilitates effective disease monitoring, ultimately aiding in preserving visual function in POAG patients.

TABLE OF CONTENTS

SL.NO.	CONTENTS	PAGE NO.
1	INTRODUCTION	1-3
2	OBJECTIVES	4
3	REVIEW OF LITERATURE	5-22
4	MATERIALS AND METHODS	23-27
5	RESULTS AND ANALYSIS	28-47
6	DISCUSSION	49-53
7	CONCLUSION	54
8	SUMMARY	55
9	BIBLIOGRAPHY	56-70
10	ANNEXURES	71-83
	Annexure I: Informed consent form	71-73
	Annexure II: Proforma	74-79
	Annexure III: Photographs	80
	Annexure IV: Master Chart	81-83

LIST OF TABLES

TABLE. NO.	DESCRIPTION	PAGE NO.
1	Subject distribution based on demographic characteristics	**29**
2	Subject distribution by different variables based on ocular examination	**32**
3	Subject distribution based on cup disc ratio	**34**
4	Distribution of subjects based on optic disc parameter (except cup disc ratio)	**35**
5	Subject distribution based on IOP measurement by Applanation tonometry	**37**
6	Distribution of study participants based on glaucomatous damage according to Hodapp-Parrish-Anderson criteria	**38**
7	Mean deviation (MD) in different glaucoma severity groups	**39**
8	Pattern standard deviation (PSD) in different glaucoma severity groups	**40**
9	Peripapillary retinal nerve fibre layer thickness in different glaucoma severity groups	**41**
10	Ganglion cell layer thickness in different glaucoma severity groups	**42**
11	Post hoc analysis between severity of glaucoma	**44**

12	Correlation between peripapillary RNFL, ganglion cell layer thickness and mean deviation in participants with Early glaucoma	**45**
13	Correlation between peripapillary RNFL, ganglion cell layer thickness and mean deviation in participants with Moderate glaucoma	**46**
14	Correlation between peripapillary RNFL, ganglion cell layer thickness and mean deviation in participants with Advanced glaucoma	**47**

LIST OF GRAPHS

FIGURE NO.	DESCRIPTION	PAGE NO.
1	Subject distribution based on age group	**30**
2	Subject distribution based on sex	**30**
3	Distribution of study participants based on presentation of family history	**31**
4	Distribution of study participants based on comorbidities	**31**
5	Distribution of study participants based on visual acuity	**32**
6	Distribution of study participants based on best corrected visual acuity (BCVA)	**33**
7	Distribution of study participants based on RAPD	**33**
8	Distribution of study participants based on cup disc ratio	**34**
9	Subject distribution based on optic disc evaluation parameters (other than cup disc ratio)	**36**
10	Subject distribution based on glaucomatous damage according to the Hodapp-Parrish-Anderson scale	**38**
11	Mean PDS of study participants	**40**

12	Mean GCL-superior thickness of study participants	**42**
13	Mean GCL-inferior thickness of study participants	**43**

LIST OF FIGURES

S.No	DESCRIPTION	PAGE NO
1	Retinal and optic nerve head anatomy as visualised by OCT	**8**
2	OCT scan for glaucoma diagnosis	**13**

LIST OF PHOTOS

PHOTOS	PHOTOGRAPHS	PAGE NO.
1	Assessment of optic nerve head with 90D and slit lamp biomicroscopy	**79**
2	Measurement of IOP by Applanation Tonometry	**79**
3	Visual field analysis with Humphery's field analyser	**79**
4	RNFL and GCL analysis with spectral domain OCT	**79**

INTRODUCTION

Glaucoma is a chronic, progressive optic neuropathy that represents a significant global health burden, affecting millions of people worldwide and leading to irreversible blindness if untreated. Primary open-angle glaucoma (POAG) is the most prevalent form of glaucoma and is characterized by an open anterior chamber angle, progressive optic nerve damage, and corresponding visual field defects. Despite its well-documented pathophysiology, the exact mechanisms underlying POAG remains incompletely understood. Nonetheless, there is mounting evidence that the loss and malfunctioning of retinal ganglion cells (RGCs) are crucial to the development of the disease. Through the optic nerve, the retinal ganglion cells carry visual information from the retina to the brain, making them essential neuronal elements of the visual pathway. The retinal nerve fiber layer (RNFL), which comprises the ganglion cells' axons, converges at the optic nerve head (ONH). In glaucoma, these cells are vulnerable to damage, resulting in structural and functional impairments that manifest as thinning of the RNFL and associated visual field (VF) defects. Thus, precise evaluation of RGC health is essential for the early diagnosis and management of glaucoma.

At present, optic nerve head (ONH) and retinal nerve fibre layers changes along with visual field defects and raised intraocular pressure (IOP) are used for diagnosis of POAG. An important diagnostic tool for assessing the visual field changes in patients with POAG is the Humphrey Visual Field (HVF) analysis. Determining the topography of the island of vision is the goal of visual field analysis to identify any deviation from the normal. Visual field assessment is conducted by adapting the eye to a specific background luminance and then presenting a stimulus of

higher brightness at various locations within the field. The patient's ability to detect this stimulus is evaluated using kinetic, static, or a combination of both. The 24-2 and 30-2 SITA Standard programs of the HFA are most frequently utilized for the diagnosis of POAG.

In visual field testing, mean deviation (MD) represents the average deviation from normal values across all tested points in a patient's visual field, indicating the overall level of visual field loss, whereas pattern standard deviation (PSD) measures the irregularity or localized pattern of that loss. The combined information derived from these is valuable for the diagnosing POAG, severity assessment and long-term disease monitoring.

Spectral domain optical coherence tomography (SD-OCT) has become a valuable imaging technique for non-invasive retinal structural visualization. It provides detailed high-resolution cross-sectional images of the retinal nerve fiber layer (RNFL) and ganglion cell layer. This enables clinical practitioners to identify structural changes linked with glaucomatous damage, particularly in its early phases and track POAG's long-term development.

The importance of early detection in POAG cannot be overstated. As much of the structural damage precedes detectable functional loss, SD-OCT serves as an valuable tool for identifying early glaucomatous changes, enabling timely intervention to preserve vision. Furthermore, detailed analysis of the macular ganglion cell-inner plexiform layer (GC-IPL) may offer additional diagnostic advantages, as the macula contains a high density of RGCs, making it highly sensitive to early damage.

This research work aims to evaluate the extent of RGC damage in patients with POAG by assessing peripapillary RNFL and macular GC-IPL thickness using

SD-OCT. Additionally, it seeks to correlate these structural changes with VF defects determined by HFA, providing a comprehensive understanding of the structural-functional relationship in glaucoma. Such insights could enhance the accuracy of glaucoma diagnosis and the efficacy of monitoring disease progression.

This study presents the stage for a thorough investigation into the structural and functional dynamics of glaucoma. By leveraging advanced imaging techniques, this research aims to contribute to the emerging body of knowledge on glaucoma pathophysiology and to improve the care of affected individuals.

AIMS AND OBJECTIVES

PRIMARY OBJECTIVE

- To evaluate the damage in retinal ganglion cells in patients with primary open angle glaucoma by assessing the peripapillary retinal nerve fibre layer and macular ganglion cell layer thickness using spectral domain optical coherence tomography

SECONDARY OBJECTIVE

- To correlate the findings of visual fields with structural changes like peripapillary RNFL and macular GC IPL thickness in patients with POAG.

REVIEW OF LITERATURE

Glaucoma-like eye diseases have been recognized since ancient Greece. Aristotle and Hippocrates used the name "glaukos" about 500 BC to refer to a late-stage disorder in which the pupil discolours grey, green, and blue. Galen (c. 129–199 AD) advanced the understanding of this condition, linking the discolouration to a forward-shifted lens, a shallow anterior chamber, and/or inadequate aqueous humor—characteristics that are quite comparable to those of contemporary descriptions of angle-closure glaucoma. In the 10th century, Al-Tabari, an Arab physician, quoted The Book of Hippocratic Treatment with relation to intraocular pressure (IOP). However, medieval Europe mischaracterized glaucoma as an incurable "green cataract" (*viriditas*), or a "waterfall," attributing it to an excessively hardened lens.

The confusion persisted for centuries, as lens removal sometimes restored vision, obscuring the role of IOP. In the middle of the 19th century, Dutch ophthalmologist Franciscus Cornelius Donders, who created the first tonometer, re-examined the link to intraocular pressure. Albrecht von Graefe (Germany) and Antoine-Pierre Demours (France) made further progress by connecting iridocorneal dysfunction to glaucoma. The concept of glaucoma was finally codified by Scottish ophthalmologist William Mackenzie in his Practical Treatise of the Diseases of the Eye (1853). It's interesting to note that certain languages, including Slovenian, still use the medieval name "green cataract." [1].

Globally, glaucoma is the leading cause of permanent blindness. The progressive deterioration of retinal ganglion cells (RGCs) is its defining feature, which is demonstrated as spatially unique visual field (VF) loss patterns that match the RGC axon bundle organization. [2] This multifactorial disease is primarily

influenced by raised intraocular pressure (IOP), a significant and alterable risk factor that influences its beginning and advancement. [3, 4] Other risk factors, include advanced age, myopia, and vascular dysfunction, also contribute significantly to the illness process, as recent genome-wide association studies have shown. [5-9]

Globally, an estimated 80 million people were affected by glaucoma in 2020, a number projected to exceed 100 million by 2040 due to the aging population. [10] Patient's quality of life (QOL) is greatly diminished by glaucoma and other vision-threatening conditions, which also raise the risk of fractures, depression, and functional impairments, exacerbating the global economic pressure. [11, 12] As a result, prompt treatment measures depend on early identification and tracking of glaucoma development, which can help slow the disease's progression and provide substantial advantages to health and the economy.

A key component of glaucoma diagnosis and treatment is optical coherence tomography (OCT) imaging. [13–15] This non-invasive technology provides objective measurements of structural changes essential for understanding and identifying glaucoma pathology. From the anterior segment, which includes the iridocorneal angle, to the posterior segment, which includes the retinal nerve fiber layer (RNFL), macula, and optic nerve head (ONH), OCT enables thorough imaging. OCT technology has recently improved picture quality, segmentation accuracy, and diagnostic algorithms while increasing scan speeds and decreasing acquisition times. These improvements enhance the precision and reproducibility of measurements, facilitating early detection and improved tracking of the course of glaucoma. Additionally, deeper structures inside the ONH, including the lamina cribrosa (LC), may now be seen because of technological advancements in OCT, which is deemed crucial to glaucoma pathophysiology. However, despite its potential, the clinical

application of quantitative LC morphometrics—such as evaluations of the beam width, pore size, microarchitecture, depth, and form—remains limited in glaucoma diagnosis and monitoring. [16]

The superficial, middle, and deep capillary plexuses are among the microvascular networks inside the retina and optic nerve head that may be seen using optical coherence tomography angiography (OCTA), a recently approved noninvasive technique. [17,18] Devices like commercial OCTA, now offer quantifiable measurements, such as vascular density, to evaluate the integrity of capillary networks within these plexuses. Studies utilizing OCTA have provided growing evidence that glaucomatous eyes exhibit abnormalities in retinal and choroidal vascular systems, potentially even at onset of the illness.

The Retina and Optic Nerve Head Anatomy concerning OCT/OCTA Glaucoma Detection

Light entering the eye is detected by photoreceptors in the neural retina, which transform it into electrochemical impulses. Bipolar cells transmit these impulses to retinal ganglion cells (RGCs) in the inner retina, with lateral inhibition by amacrine and horizontal cells illustrated in Figure 1A. The optic nerve head is where RGC axons converge, pass through scleral canal, and exit the

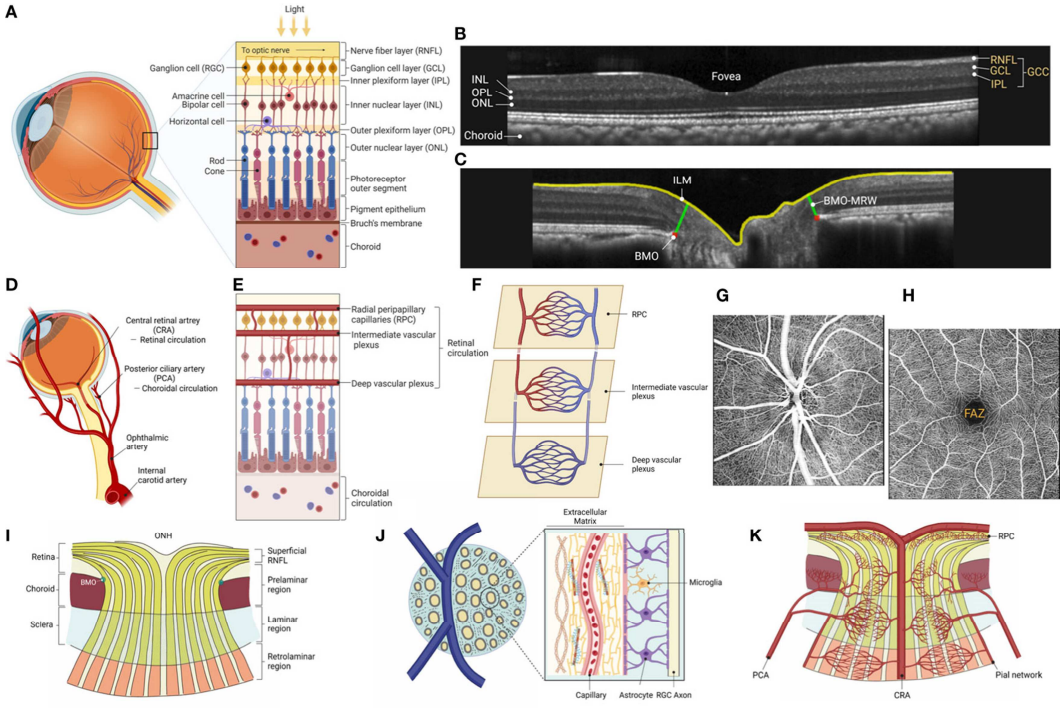

Figure 1: Retinal and Optic Nerve Head Anatomy as Visualized by OCT

Source: https://www.frontiersin.org/files/Articles/1217125/fopht-03-1217125-HTML/image_m/fopht-03-1217125-g001.jpg

Eye to form the Optic Nerve. Retinal ganglion cell axons cross to contralateral hemisphere at the optic chiasm and then synapse in the midbrain, including the lateral geniculate nucleus. RGC death disrupts vision and other physiological functions, like circadian rhythms. [19] Advanced OCT technology enables detailed visualization of the retina and ONH, aiding in glaucoma diagnostics. [20] The central retina, with cone-dominated photoreceptors, has thicker layers (IPL and GCL) than the peripheral retina, which is rod-dominated. These layers play a key role in pathophysiology of glaucoma, particularly the Ganglion Cell-Inner Plexiform Layer (GCIPL) and Ganglion Cell Complex (GCC) depicted in Figure 1B. [20,21]

OCTA Reveals Distinct Layers of the Retinal Capillary Network

Investigations using spectral domain optical coherence tomography (SD-OCT) have highlighted the significance of inner macular layer thickness in detecting early structural damage associated with glaucoma. The macular ganglion cell layer (GCL) contains more than half of the retinal ganglion cells. Two inner macular layers that physically resemble the peripapillary region are the retinal nerve fiber layer (RNFL) and GCL. Thus, the three deepest macular retinal layers that comprise the ganglion cell complex are the retinal nerve fibre layer, ganglion cell layer, and inner plexiform layer. [21]

The diagnostic value of macular GCL+IPL thickness features in early glaucoma has been shown in several studies. [22,23,24] Measurements of GCL+IPL thickness, both average and minimum, have shown improved specificity and sensitivity in identifying initial glaucoma as opposed to advanced stages. [22] It was reported by Mwanza et al. that minimum ganglion cell layer and inner plexiform layer thickness was the most reliable indicator for detecting early glaucoma throughout the perimetric and pre-perimetric phases. [24] The study also showed that the most sensitive sectors for early glaucoma diagnosis were the GCL+IPL thickness sectors in the inferior macular and inferotemporal regions. Studies have reported a strong relationship between RNFL characteristics and GCL+IPL in identifying glaucoma-related structural damage. According to the results, both structural criteria are equally useful in identifying glaucoma in its early stages, and several studies advise using them in tandem for diagnosis. [25] Recently, there has been growing interest in utilizing both parameters for the diagnosis and glaucoma monitoring.

The Cirrus® SD-OCT's new function merges the macular cube and optic disc cube scans into a single picture. Correlating changes in the RNFL and macular GCL + IPL is made easier by the PanoMap®, an integrated widefield RNFL and macular thickness and deviation map, which may make glaucomatous pattern recognition easier. [25] Recent research employing PanoMap® has concentrated on the pre perimetric as well as on perimetric phases in early disease development and baseline damage. [21,25] These studies have shown that in the early stages of glaucoma, macular regions are more likely than peripapillary areas to have glaucomatous structural damage.

A division of the internal carotid artery is the ophthalmic artery, is a source of the retinal and choroidal vasculatures, two separate circulatory systems that nourish the human retina, shown in Figure 4D. The central retinal artery (CRA) supplies blood to the retinal vasculature, which divides into quadrants at the ONH. This feeds the inner retina, which includes the IPL, GCL, and RNFL, whereas the choroidal circulation supports the outer retina, mainly the photoreceptors. [26] Retinal arteries deliver blood to three distinct capillary networks within the retina: the superficial, middle, and deep. Specifically, the retinal nerve fiber layer receives blood supply from the optic nerve head's (ONH) radial peripapillary capillary (RPC) plexus, and macula features a specialized superficial capillary layer that is visualized with the help of Optical Coherence Tomography Angiography (OCTA). [27, 28] The deep vascular plexus receives blood indirectly through intermediate plexus anastomoses and the fovea contains a capillary-free FAZ within peri-foveal capillaries as described in Figure 4H. [29, 30]

Ciliary arteries that branch into Haller's and Sattler's layers supply the choroid, which is heavily vascularized to sustain the outer retina. These arteries end at the choriocapillaris, which is close to Bruch's membrane. [31, 32] Lamina cribrosa obtains its blood supply from the circle of Zinn-Haller, though its variability increases vulnerability to ischemia. [33] Choroidal venous drainage occurs through vortex veins. Physiologically, choroidal vessels are autonomically regulated, whereas the retinal vasculature relies on endothelial cells, pericytes, and astrocytes for autoregulatory processes. [34]

Generation of OCT in glaucoma

Optical Coherence Tomography uses low-coherence interferometry to measure how light bounces off the retina's internal structures to produce detailed, cross-sectional pictures of the retina. [35] Commercially, at least three generations of OCT are available, with each generation improving scan speed, image quality, The clarity of the image (SNR) and the ability to see fine details deep within tissues.

Time Domain OCT

By comparing it to the round-trip optical path length of a reference beam, the first generation, TD-OCT, determines the axial depth of near-infrared light backscattered from the retina. This process involves mechanical modulation of a mirror to scan depth positions sequentially, reconstructing the reflectivity profile at every location. The mechanical mirror displacement limits the maximum scanning speed to 400 A-scans/second. [36]

Spectral Domain OCT

One type of Fourier domain OCT (FD-OCT) is the second-generation SD-OCT, that employs near-infrared light centered at 850 nm. [37] SD-OCT determines the tissue's depth structure by analyzing the frequency components of the reflected light, rather than physically scanning a beam. This approach significantly increases scanning speed to over 100,000 A-scans/second in current devices, reducing acquisition time and improving image quality and SNR. However, SD-OCT experiences signal roll-off, where signal strength diminishes with increasing depth, limiting its performance. [38]

Swept Source OCT

Another FD-OCT is swept source OCT that achieves scanning speeds of 200,000 or more A-scans/second in current commercial systems. [39] Instead of a spectrometer, the system employs a rapidly sweeping narrowband laser and a fast photodetector to record spectral interference patterns across a broad range of frequencies. Around 1050 nm is the core wavelength at which it operates and minimizes signal roll-off and scattering, allowing imaging of deeper structures like the LC. While offering high-speed scanning and deep tissue imaging, due to its longer wavelength, it has a reduced resolution.

Glaucoma Diagnosis Using optical coherence tomography

The use of Spectral-Domain Optical Coherence Tomography (SD-OCT) has transformed the diagnosis of glaucoma by providing accurate, quantifiable assessment of critical structural components of the eye, from the retinal nerve fibers to deep optic

nerve head structures. Despite its high diagnostic accuracy, early-stage glaucoma detection and assessment in highly myopic eyes remain challenging.

Measurements of the global and inferior-sector average circumpapillary retinal nerve fibre layer thickness, the latter of which is more vulnerable to glaucomatous damage, are used because of their diagnostic accuracy and are frequently utilized. (sensitivity: 60–98%; specificity: 80–95%) described in Figures 2 A, B. [40-42]

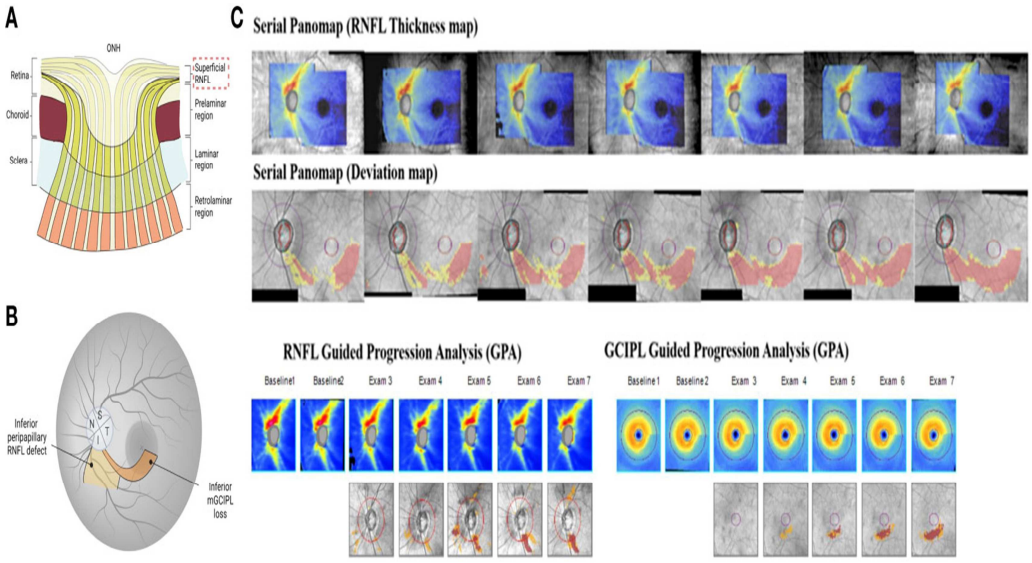

Figure: 2 OCT Scan for glaucoma diagnosis

Source:https://www.frontiersin.org/files/Articles/1217125/fopht-03-1217125-HTML/image_m/fopht-03-1217125-g002.jpg

Research indicates that mean cpRNFL thickness can identify glaucomatous damage years before visual field defects manifest. For example, a study discovered that 19% of eyes had abnormalities eight years before VF defect identification, while 35% of eyes had aberrant cpRNFL thickness four years before highlighting how crucial cpRNFL measurements are for early detection. [43]

However, depending on the abnormality threshold the sensitivity of OCT parameters in preperimetric glaucoma varies from 21.0% to 87.1%. [44] However, individual ONH structural abnormalities, like peripapillary atrophy and tilted discs, which are frequent in myopic eyes, might affect cpRNFL thickness. When macular and retinal diseases are absent, macular imaging provides a more stable and less variable structural profile across individuals. [45] Macular retinal ganglion cell damage, comprising macular retinal nerve fibre layer, ganglion cell-inner plexiform layer and ganglion cell complex, may be specifically quantified using the macular inner retinal layer segmentation. Among these metrics, GCC and GCIPL are especially useful for differentiating between glaucoma-affected and healthy eyes at various stages of the condition, including preperimetric stages. [46, 47] According to a prior study, the best metric for identifying glaucoma in myopic eyes is the inferotemporal GCIPL thickness shown in Figure 2B. [48] Furthermore, asymmetry is frequently seen in early glaucomatous damage. Even in very myopic eyes with tessellated fundus, where RNFL abnormalities are less noticeable, automated identification of hemifield disparities in GCIPL thickness across the horizontal raphe may accurately detect early structural damage. [49]

With advancements in scanning speed, modern **swept-source OCT (SS-OCT)** devices can cover larger areas in a single scan, eliminating the need for separate scans of the Optic Disc as well as macula. A single volumetric modality, encompassing peripapillary Optic nerve head and macular regions, allows for complete visualization, facilitating the early identification of glaucomatous alterations and the accurate localization of retinal nerve fibre layer abnormalities. [50]

OCT 3D volume scans may be used to determine optic nerve head metrics such as rim area, rim thickness and cup-to-disc ratio. The bruch's membrane opening minimum rim width (BMO-MRW), or the smallest gap between the BMO and the inner limiting membrane, is a sensitive and reproducible metric for early glaucoma detection. [51] Similarly, the distance between the vitreoretinal interface and the BMO, or 3D neuroretinal rim thickness, improves diagnostic precision, particularly in reducing false positives in myopic eyes. [52]

Since glaucoma-related structural damage may only be apparent with specific diagnostic parameters, combining information from ONH, cpRNFL and macular scans can enhance accuracy in detecting glaucoma depicted in Figure 5B. [53, 54]

The literature analysis concludes by highlighting the complex connection between functional visual field abnormalities and anatomical alterations in the retina in individuals with primary open-angle glaucoma (POAG). Studies consistently emphasize the diagnostic utility of measuring macular ganglion cell layer-inner plexiform layer thickness and peripapillary retinal nerve fiber layer thickness as sensitive biomarkers for early glaucomatous damage. These parameters correlate significantly with visual field changes, offering a thorough comprehension of the course of the glaucoma. The incorporation of structural and functional assessments underscores the importance of advanced imaging technologies like optical coherence tomography (OCT) in glaucoma management. Further research is essential to refine these correlations and explore their implications in enhancing the predictive accuracy and therapeutic strategies for POAG.

OCT-based glaucoma detection and progression tracking

Optical coherence tomography (OCT) is essential for the early diagnosis and tracking of glaucoma development in order to avoid permanent retinal ganglion cell (RGC) damage and vision loss. Studies have shown that OCT is reliable in diagnosing disease progression; nevertheless, variables such as disease severity, variability in progression, and age-related changes affect OCT's prediction accuracy. [55]

By integrating functional and structural data, a Bayesian modeling technique has been demonstrated to increase sensitivity and specificity in identifying glaucoma worsening, beating conventional linear regression models. [56] Due to their long-term reliability, measures such as the circumpapillary retinal nerve fiber layer (cpRNFL) and the thickness of the macular ganglion cell-inner plexiform layer (GCIPL) have been used successfully in progression algorithms. [57] In advanced glaucoma, cpRNFL thickness may become less sensitive due to the 'floor effect,' where remaining tissue reaches the measurable limit, making it less effective for detecting further progression. [58, 59] Two studies on advanced glaucomatous eyes have shown no significant difference in cpRNFL thickness changes between visual field (VF) progressors and non-progressors, suggesting that cpRNFL may not be sensitive enough in advanced stages. [60, 61]

In contrast, GCIPL evaluation offers greater sensitivity in detecting progression, even in advanced glaucoma, since there is less chance of the floor effect. A study comparing GCIPL thinning rates found that those with glaucoma progression showed significantly faster GCIPL thinning than non-progressors, indicating that GCIPL thickness on OCT may be an effective objective marker for progression. [62] Longitudinal studies have further demonstrated that GCIPL thinning occurs before

cpRNFL thinning in early glaucoma, suggesting that GCIPL changes can precede RNFL damage. [63] Therefore, combining cpRNFL and GCIPL measurements provides a comprehensive approach to early detection of glaucoma progression. [64]

Wide-field swept-source OCT (SS-OCT) imaging offers additional advantages, allowing for comprehensive measurements of both the macular and peripapillary regions, thereby enhancing the detection of structural changes in glaucoma. [65] The integration of OCT scans with VF data, as seen in recent advancements such as the one-page report developed by Hood et al., can facilitate the visualization of structure-function relationships and improve disease progression predictions. [66] To properly evaluate the clinical use of wide-field SS-OCT in identifying progression, more longitudinal investigations are required. Furthermore, a region-of-interest method that monitors the growth of RNFL defects can successfully identify advancement in these areas in instances with focal RNFL abnormalities. [67]

Finally, according to current studies on beta-zone peripapillary chorioretinal atrophy, OCT can detect peripapillary atrophy subtypes that can be useful in forecasting the course of glaucoma. Beta zone peripapillary atrophy affected eyes lose structure and function more quickly than those with gamma-zone PPA or without PPA, providing new insights into progression risk. [68] Thus, the combination of OCT's ability to detect both structural changes and specific ocular features like beta-zone PPA holds promise for advancing glaucoma monitoring and intervention strategies.

Previous studies:

Abd El-Naby et al. (2018) analyzed 80 eyes (20 healthy, 60 with glaucoma of varying severity) using optical coherence tomography (OCT). They discovered that

average retinal nerve fiber layer (RNFL) thickness was a strong indicator of glaucoma, with progressive thinning correlating to increasing disease severity. Specifically, early glaucoma showed a 14.9% RNFL reduction, moderate glaucoma a 25.1% reduction, and severe glaucoma a 37.2% reduction. The research demonstrated a strong link between RNFL thickness and visual field loss, suggesting that average RNFL thickness is a valuable tool for diagnosing and staging glaucoma. [69]

Hou et al. (2018) found that glaucoma progression analysis (GPA) detected thinning in the macular ganglion cell-inner plexiform layer (GCIPL) and retinal nerve fiber layer (RNFL) with high specificity. GCIPL thinning was observed in 24.7% of eyes, and RNFL thinning in 28.6%. Importantly, GCIPL thinning significantly increased the risk of subsequent RNFL thinning (and vice versa), suggesting a strong predictive relationship between these two parameters. Both GCIPL and RNFL thinning were also associated with an increased risk of visual field (VF) progression. However, VF progression itself did not significantly predict GCIPL or RNFL thinning. These results highlight the value of monitoring both GCIPL and RNFL for early detection of glaucoma progression, as they independently and mutually predict future damage and VF loss. [70]

Lin et al. (2018) found no significant differences in peripapillary retinal nerve fiber layer (pRNFL), total macular layer (TML), or inner macular layer (IML) thickness between patients with primary open-angle glaucoma (POAG) and normal-tension glaucoma (NTG). However, macular ganglion cell layer (mGCL) thickness in the superior and inferior regions significantly correlated with visual field loss and pRNFL thickness. Notably, the inferior-outer sector of the macula showed superior diagnostic performance compared to the inferior-inner sector. The diagnostic accuracy of mGCL thickness was comparable to pRNFL thickness for detecting early

glaucoma, with global pRNFL showing the highest sensitivity, followed by the inferior-outer mGCL. This suggests that mGCL measurements, especially in the inferior-outer macula, are valuable for early glaucoma detection, similar to pRNFL. [71]

Deshpande et al. (2019) demonstrated that both ganglion cell-inner plexiform layer (GCL-IPL) and retinal nerve fiber layer (RNFL) parameters can effectively differentiate between normal eyes, pre-perimetric glaucoma (PPG), and perimetric glaucoma. Specifically, the inferotemporal GCL-IPL region was most accurate for classifying perimetric glaucoma, while the inferior GCL-IPL was best for detecting PPG. For RNFL, the inferior thickness was strongest for distinguishing POAG from normal eyes, and average RNFL was best for differentiating POAG from PPG. While RNFL measurements showed slightly higher diagnostic accuracy than GCL-IPL, especially in detecting PPG and perimetric glaucoma, the differences were small and may not be clinically significant. Notably, both GCL-IPL and RNFL showed high sensitivity but low specificity when differentiating perimetric glaucoma from PPG. [72]

Ustaoglu et al. (2019) found that ganglion cell-inner plexiform layer (GC-IPL) parameters effectively distinguished between healthy eyes, glaucoma suspects, and different glaucoma stages. Notably, GC-IPL parameters, particularly minimum, inferotemporal, and inferonasal thicknesses, were able to differentiate early glaucoma from glaucoma suspects, a distinction that retinal nerve fiber layer (RNFL) and optic nerve head (ONH) parameters could not make. While RNFL and the average cup-to-disc (c/d) ratio performed well in separating healthy eyes from suspects, GC-IPL parameters were crucial for differentiating early glaucoma. GC-IPL parameters, especially the minimum thickness, also showed high accuracy in distinguishing moderate-to-severe glaucoma from early glaucoma, performing comparably to RNFL

and rim area measurements. Overall, GC-IPL parameters are reliable for detecting and staging glaucoma, demonstrating similar diagnostic performance to other established methods. [73]

Xu et al. (2020) found no significant differences in OCT thickness parameters between normal-tension glaucoma (NTG) and primary open-angle glaucoma (POAG) groups. When distinguishing either NTG or POAG from healthy eyes, average and inferior retinal nerve fiber layer (RNFL) thickness, along with minimum ganglion cell-inner plexiform layer (GCIPL) thickness, showed the best diagnostic performance. Notably, the diagnostic accuracy of minimum GCIPL thickness was comparable to that of the best-performing RNFL parameters in both NTG and POAG. However localized GCIPL thinning, particularly in the inferior and inferotemporal sectors, was more common in NTG than POAG. This study suggests that minimum GCIPL thickness is as effective as average and inferior RNFL thickness in differentiating glaucoma from normal eyes, regardless of whether it's NTG or POAG. [74]

Gupta et al. (2021) examined 77 eyes from 40 POAG patients, finding a clear correlation between glaucoma severity and thinning of both peripapillary RNFL and macular GCL-IPL. In early glaucoma, superior RNFL thinning was prevalent, while advanced glaucoma showed significant thinning in the inferior RNFL. Progressive thinning of the inferior GCL-IPL was also observed with increasing disease severity. Both RNFL and GCL-IPL thicknesses correlated positively with visual field mean deviation across all stages. The study highlights the importance of assessing RNFL and GCL-IPL alongside visual field defects for accurate POAG progression monitoring. Furthermore, GCL-IPL thickness changes strongly reflected visual

function and RNFL structure alterations, making it a crucial parameter in glaucoma evaluation. [75]

Bhat et al. (2022) found a progressive loss of retinal nerve fiber layer (RNFL) thickness with increasing severity of primary open-angle glaucoma (POAG), with average losses of 25.44%, 29.67%, and 44.15% in mild, moderate, and severe stages, respectively. RNFL loss significantly correlated with glaucoma severity in most sectors, and negatively correlated with visual field index (VFI) in many sectors, except in certain regions of moderate and severe POAG. Mean deviation (MD) showed a significant positive correlation with RNFL loss, particularly in the temporal-inferior (TI) sector of mild POAG and across all sectors in severe POAG. The study concludes that RNFL thickness is a reliable indicator of POAG severity, and that the temporal-inferior and nasal-inferior sectors are most vulnerable to glaucomatous damage. [76]

Rabiolo et al. (2022) found that both spectral-domain OCT (SD-OCT) and swept-source OCT (SS-OCT) showed significant thinning of peripapillary retinal nerve fiber layer (pRNFL) and macular ganglion cell-inner plexiform layer (mGCIPL) in glaucoma patients compared to healthy controls and glaucoma suspects. While the two OCT techniques showed a strong correlation in most areas, some differences were observed in the nasal and temporal pRNFL quadrants. The study noted a proportional bias between the devices' measurements, which could be adjusted with conversion formulas. Although the thickness values weren't directly interchangeable, they were interconvertible. Importantly, both SD-OCT and SS-OCT showed similar diagnostic accuracy in differentiating glaucoma patients from suspects and healthy individuals. [77]

Luttrull et al. (2024) found that adding vibratory photothermal therapy (VPT) to standard open-angle glaucoma (OAG) management significantly improved nerve fiber layer (NFL) and ganglion cell complex (GCC) trends. Specifically, a much higher percentage of VPT-treated eyes showed positive NFL and GCC trends compared to control eyes. The mean NFL trend shifted from a decrease in control eyes to an increase in VPT-treated eyes, and the mean GCC trend showed a significantly smaller decrease in VPT-treated eyes. These results suggest that VPT can potentially reverse critical indicators of glaucoma severity and progression. [78]

San Pedro et al. (2024) found that both ganglion cell plus inner plexiform layer (GCL+IPL) and circumpapillary retinal nerve fiber layer (cRNFL) thicknesses decreased with increasing glaucoma severity in a study of 122 eyes. For detecting visual field defects, the minimum GCL+IPL thickness was most effective. Average GCL+IPL was best for identifying progression from glaucoma suspect to mild glaucoma, while inferior cRNFL was strongest for distinguishing mild from moderate-to-severe glaucoma. The study highlights the value of macular ganglion cell analysis in glaucoma screening, detection, and staging, especially for early detection and progression, where it outperformed cRNFL. [79]

MATERIALS AND METHODS

Study design

The present research work was a hospital-based observational cross-sectional study.

Study duration

The study was conducted for a period of one year from April 2023 to March 2024.

Study population

The study population consisted of patients attending Department of Ophthalmology, KLE's Dr Prabhakar Kore Hospital and Medical Research Centre during the study period fulfilling the inclusion criteria and consenting to participate in the study.

Selection criteria

Inclusion criteria:

- All patients above the age of 18 years diagnosed with primary open angle glaucoma.

Exclusion criteria:

- Best corrected visual acuity (BCVA) <20/40
- Patients with any ocular disease or treatment that could independently affect retinal thickness or visual-fields, such as:

✓ Significant ocular media opacities

- ✓ Anterior segment anomalies (example: aniridia)
- ✓ History of intraocular surgery (example: cataract)
- ✓ Secondary glaucomas
- ✓ Diabetic retinopathy

Sample size

The minimum sample size was obtained by the formula based on prevalence rate as given below:

$$n = \frac{z_\alpha^2 \, P(1-P)}{d^2}$$

Where:

n = sample size

Z_α = linked with the level of significance.

In this study, for 5% level of the significance $Z_\alpha = 1.96$

P = the prevalence rate of early and moderate glaucoma eyes among the glaucoma patients, which is 74% for this study

d = percentage likely difference in the prevalence.

In this study, d = 20% of P, which is equal to 14.80%

Based on the above parameters, the minimum sample size was estimated to be 34.

Sampling procedure

Convenient sampling method was adopted for this study.

Data collection procedure

After obtaining the approval from the institutional review board and Institutional Ethics committee, patients attending the Department of Ophthalmology, KLE's Dr Prabhakar Kore Hospital and Medical Research Centre, Belagavi who satisfied the above-mentioned criteria were enrolled into the study. Consent was taken from all participants after thoroughly explaining the tests they would be subjected to in this study and providing all the information regarding the same.

Detailed history was taken that included their demographic details, presenting symptoms, associated systemic conditions and history of past intraocular (cataract) surgery or ocular trauma.

A comprehensive ocular examination was done, including assessment of distant and near visual acuity, with Snellen's and Jaeger's chart respectively. Best Corrected Visual Acuity (BCVA) was assessed. Anterior segment evaluation was done by Haag-Streit slit lamp biomicroscope. An Opticlear four-mirror gonio lens was utilized to assess the anterior chamber angle, enabling the distinction between open and closed angle configurations. Intraocular pressure was measured with applanation tonometry.

The visual field analysis of patients was done using the Humphrey visual field analyser 3. The SITA Standard 30-2 program was performed in all participants and only reliable visual fields were taken into consideration that included fixation losses

of <33%, false positive of <20% and false negative of <20% with foveal threshold of more than 30dB.

The severity of glaucomatous damage in the study participants was categorized based on the Hodapp-Parrish-Anderson scale, determined by the mean deviation acquired from visual field analysis.

The classification comprised three stages:

Early glaucoma with mean deviation (MD) less than 6dB

Moderate glaucoma with MD between 6dB and 12dB

Advanced or Severe glaucoma indicated by an MD greater than 12dB.

The Pattern Standard Deviation (PSD) was also recorded for all participants.

Ocular dilatation was performed using tropicamide 0.8% and phenylephrine 5% eyedrops. Optic disc evaluation was done by slit lamp bio-microscopy using 90D lens. Parameters like disc size, disc margins, cup size, cup to disc ratio, laminar dot sign, bayonetting sign, notching, splinter hemorrhages, nerve fibre layer defects, neuro-retinal rim assessment and alpha and beta zones were considered. Indirect ophthalmoscopy was done to rule out any other retinal pathologies that might influence retinal thickness and consequently, visual field analysis.

Evaluation of peripapillary retinal nerve fibre layer thickness and macular ganglion cell layer thickness was performed using Topcon-Maestro 3D Spectral Domain Optical Coherence Tomography. Distinct associated variables such as retinal nerve fibre thickness (total, superior and inferior) and macular ganglion cell thickness (total, superior and inferior) were recorded.

Statistical analysis

Analysis of collected data was done using descriptive statistics. SPSS software version 21.0 and Microsoft Excel were employed for statistical analysis. Continuous quantitative variables were represented as mean ± standard deviation (SD). In cases where the data were partitioned into two distinct groups based on a qualitative attribute, Student's unpaired t-tests were employed for the analysis of continuous variables for comparative purposes.

Nonparametric tests were used for discrete variables and were represented by median (minimum, maximum) and categorical variables were presented as rates, ratios, and percentages. The relationship between outcomes, clinical factors, and demographic characteristics were evaluated using the Chi-square test. Normality of variable was checked by Shapiro Wilk test and QQ plot. If data followed normal distribution, One-way ANOVA was used for analysis. Otherwise, non-parametric test like Kruskal Wallis test was employed. Post-hoc analysis was done by Tukey’s test. Correlation between parametric variables was analyzed by Spearman rho test. For all the tests, p values<0.05 were considered as statistically significant.

RESULTS

The study was a hospital-based observational cross-sectional study conducted at the Department of Ophthalmology, KLES Dr Prabhakar Kore Hospital and Medical Research Centre, Belagavi for a period of one year after receiving approval from the Institute Ethics Committee. The study participants included patients with POAG.

A total number of 34 patients diagnosed with POAG were included in this study.

To facilitate an accurate and efficient assessment, parameters of only the right eye (OD) were analyzed.

In all patients, gonioscopy of right eye (OD) showed open angles.

Details of the demographic characteristics of the study participants are given in Table 1.

Table 1. Subject distribution based on demographic characteristics.

Variable	Subcategory	Number of study participants (%)
Age (years)	<35	1 (2.9%)
	35-50	6 (17.6%)
	51-65	14 (41.2%)
	66-80	12 (35.3%)
	>80	1 (2.9%)
	Mean ± SD	60.38 ± 12.96
	Median (Min, max)	61 (33, 84)
Sex	Female	6 (17.6%)
	Male	28 (82.4%)
Family history	Present	5 (14.7%)
	Nil	29 (85.3%)
Comorbidities	Chronic Kidney Disorder	1 (2.7%)
	Diabetes Mellitus	8 (21.6%)
	Hypertension	13 (35.1%)
	Ischemic Heart Disease	1 (2.7%)
	Nil	13 (35.1%)
	Thyroid	1 (2.7%)

The mean of age of the study participants was 60.38 ± 12.96 years. Majority of the subjects were in the age group of 51-65 years (n=14, 41.2%), followed by those in the 66-80 years age group (n=12, 35.3%), depicted in figure 1.

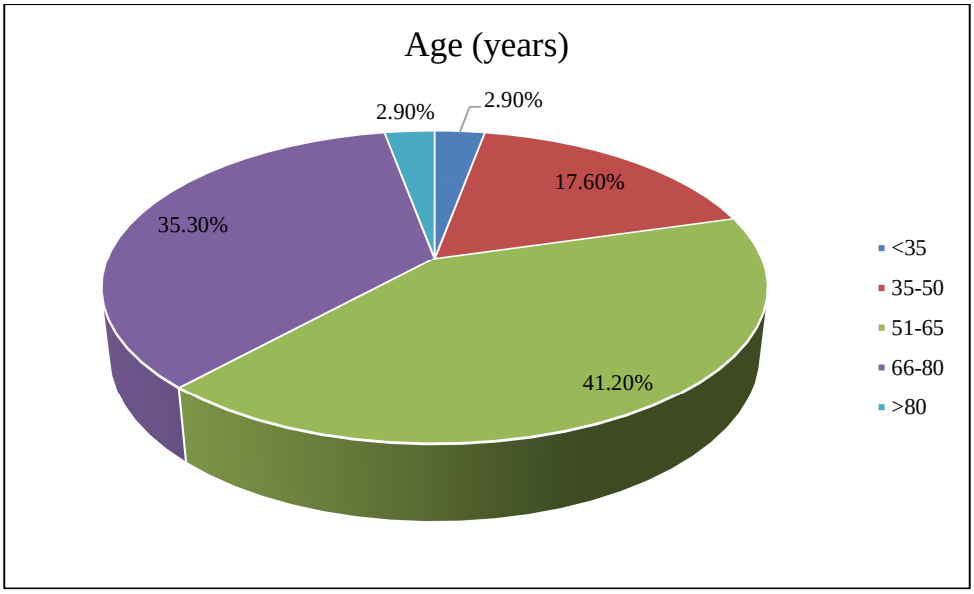

Graph 1: Subject distribution based on age group

Amongst the 34 study participants, 28 (82.4%) were males and 6 (17.6%) were females, shown in figure below.

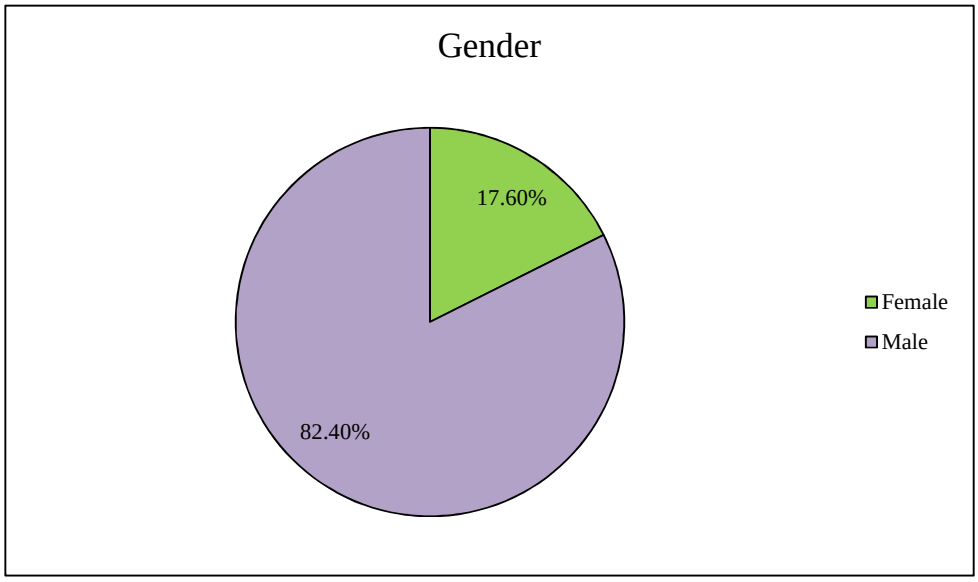

Graph 2: Subject distribution based on sex

In this study, 29 (85.3%) did not report any family history of POAG portrayed in Figure 5.

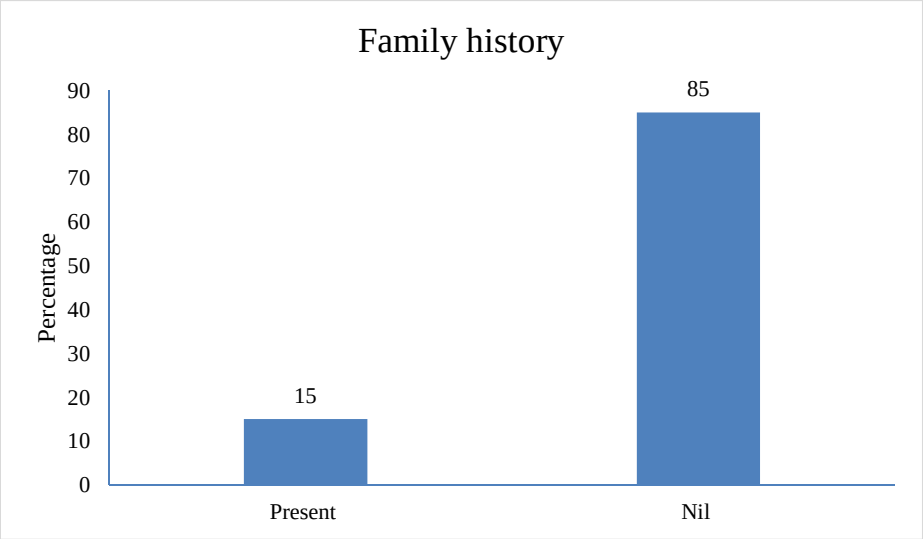

Graph 3: Distribution of study participants based on presentation of family history

The most reported comorbidity among the study participants was hypertension (35.10%), followed by diabetes mellitus (21.60%). Study participants also reported thyroid problems, ischemic heart disease, and chronic kidney disease, each at 2.70%. Around 35.10% of study participants reported no comorbidity, illustrated below.

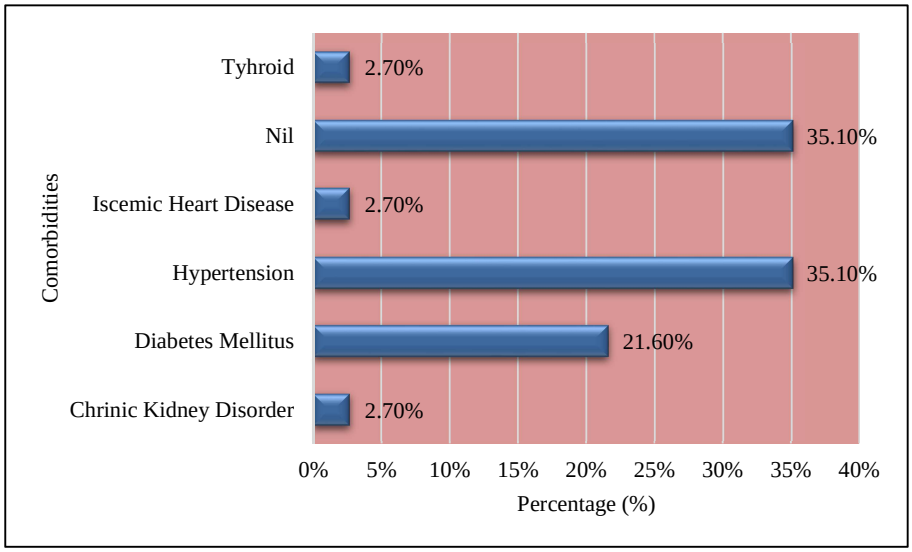

Graph 4: Distribution of study participants based on comorbidities

Ocular examination variables in the study participants are presented below.

Table 2. Subject distribution by different variables based on ocular examination

Variables	Subcategory	Ocular examination
Visual Acuity	6/6 to 6/12	17 (50%)
	6/12 to 6/60	16 (47.1%)
BCVA	6/6 to 6/9	26 (76.47%)
	6/9 to 6/12	8 (23.53%)
Pupillary reaction by swinging flash light test to detect RAPD	Present	1 (2.9%)
	Absent	33 (97.1%)

Among the study participants, visual acuity of 6/6 to 6/12 was observed in 17 (50%) subjects whereas 6/12 to 6/60 was noted in 16 (47.1%) subjects in the right eye as depicted in Figure 5.

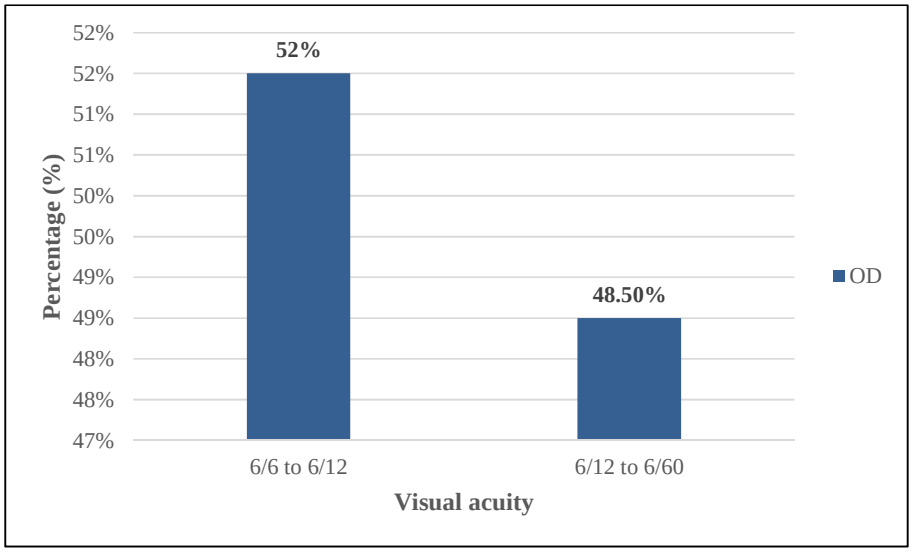

Graph 5: Distribution of study participants based on visual acuity

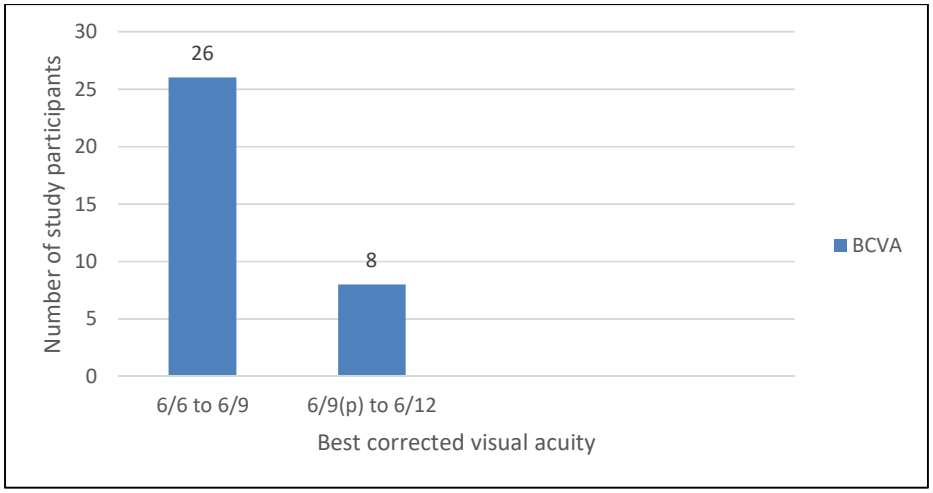

Graph 6: Distribution of study participants based on best-corrected visual acuity (BCVA)

Among the study participants, BCVA of 6/6 to 6/9 was observed in 26 (76.47%) subjects whereas 6/9 (p) to 6/12 was noted in 8 (23.53%) subjects as depicted in Figure 8

RAPD was present in one study participant, i.e., 2.9% represented in Figure 6.

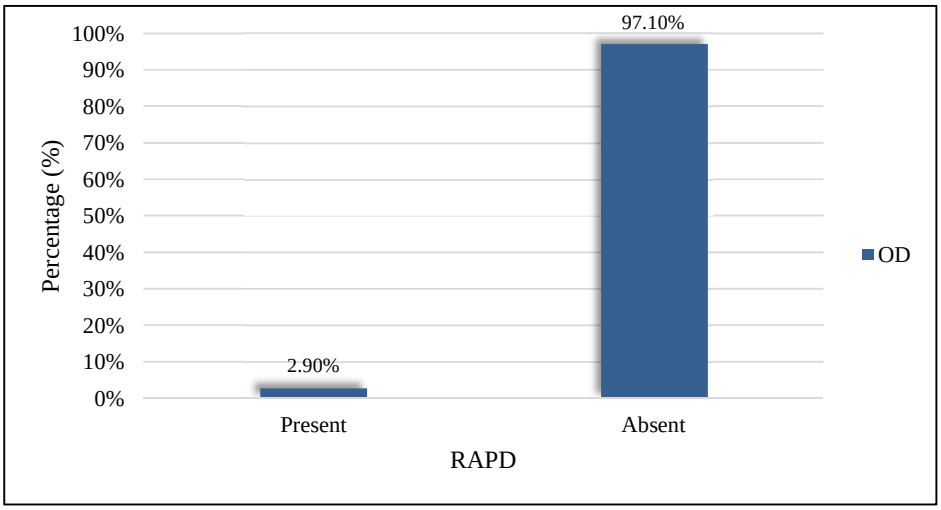

Graph 7: Distribution of study participants based on RAPD

Table given below highlights cup disc ratio of all the participants in the study group.

Table 3. Distribution based on cup-disc ratio

Variable	Range	Number of subjects (%)
Cup disc ratio	<0.3	1 (2.9%)
	0.3 to 0.6	20 (58.8%)
	0.7 to 0.9	13 (38.2%)

20 (58.8%) study participants had cup disc ratio (C:D) between 0.3 to 0.6, 13 (38.2%) had C:D between 0.7 to 0.9, as shown in the following figure.

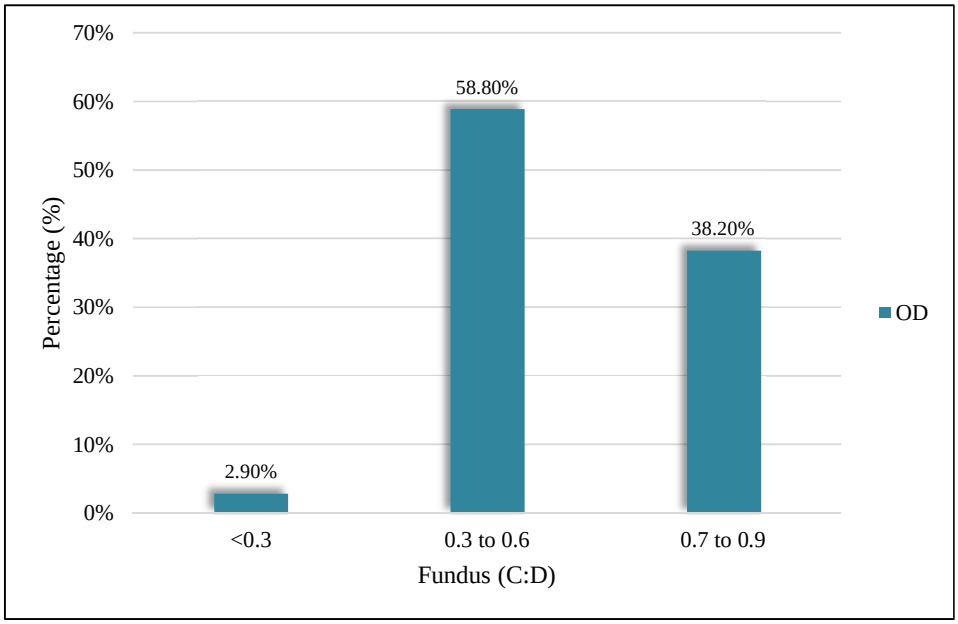

Graph 8: Distribution based on cup disc ratio (optic disc evaluation)

Distribution of subjects based on optic disc evaluation parameters other than cup disc ratio is shown below.

Table 4. Distribution based on optic disc parameters (except cup disc ratio)

Variables	Subcategory	Number (%)
Optic disc evaluation parameters in OD	Thinning of NRR	3 (16.7%)
	Splinter hemorrhages	2 (11%)
	Laminar dot sign	2 (11%)
	Bayonetting	3 (16.7%)
	Notching	1 (5.6%)
	Nasalisation of vessels	1 (5.6%)
	PPA	1 (5.6%)
	Optic atrophy	1 (5.6%)
	Others (Temporal pallor)	4 (22.2)

It can be concluded that 3 (16.7%) had Thinning of NRR, 3 (16.7%) had Bayonetting, 2 (11%) had Splinter hemorrhages, 2 (11%) had disc pallor, also illustrated in the figure 8.

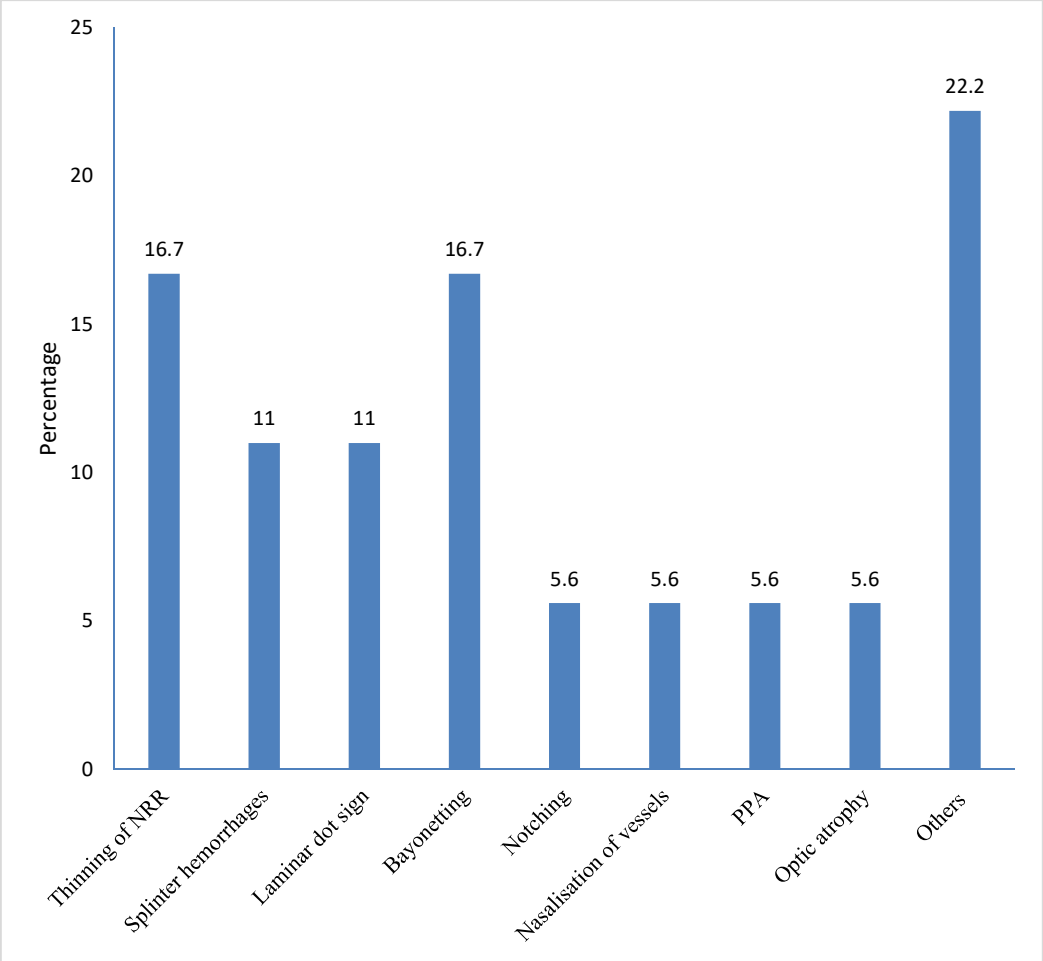

Graph 9: Subject distribution based on optic disc evaluation parameters (other than cup disc ratio)

The following table shows the distribution of study participants according to the IOP measurement in the right eye (OD) using Applanation Tonometry (AT).

Table 5. Subject distribution based on IOP measurement by AT (RE)

Variable	Subcategory	Glaucoma Severity OD
IOP by AT (RE)	Mean ± SD	22.1 ± 7.3
	Median (Min, max)	22 (9, 42)

The mean IOP was reported to be 22.1 ± 7.3 mm Hg by applanation tonometry (AT).

The following table depicts the categorization of subjects based on severity of glaucomatous damage.

Table 5. Distribution of study participants based on severity of glaucomatous damage according to the Hodapp-Parrish-Anderson scale.

Subcategory	Glaucoma Severity OD
Early	17 (51.5%)
Moderate	6 (18.2%)
Advanced	10 (30.3%)

Among study participants, 17 (51.5%) subjects had early glaucomatous damage, 6 (18.2%) had moderate damage and 10 (30.3%) belonged to advanced or severe group, illustrated in Figure 8.

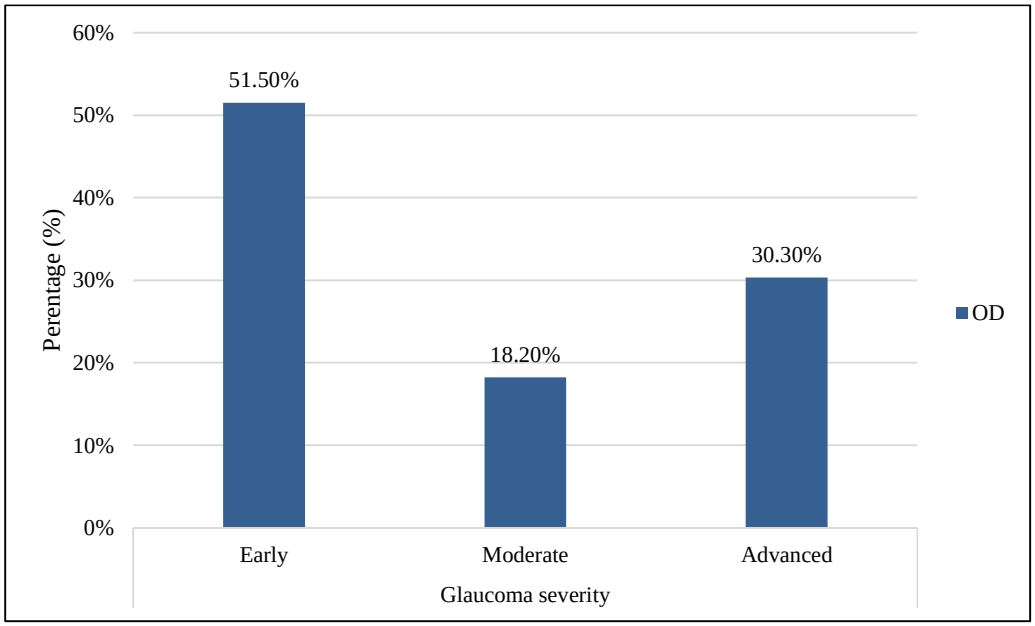

Graph 10: Subject distribution based on glaucomatous damage according to the Hodapp-Parrish-Anderson scale.

The mean deviation values obtained from visual field testing in different glaucoma severity groups are demonstrated below.

Table 6. Mean deviation (MD) in different glaucoma severity groups

Variable	Subcategory	Glaucoma Severity-OD			p-value
		Early	**Moderate**	**Advanced**	
Mean deviation (db)	Mean ± SD	-2.87 ± 1.99	-9.4 ± 2.06	-15.91 ± 14.24	<0.001*KW
	Median (Min, max)	-1.79 (-6.86, -0.83)	-9.67 (-11.56, -6.4)	-19.99 (-30.18, 21.96)	

The MD for early, moderate and advanced severity groups were determined to be -2.87 ± 1.99, -9.4 ± 2.06 and -15.91 ± 14.24, respectively.

Pattern standard deviation (PSD) values from visual field analysis in different glaucoma severity groups are presented below.

Table 7. Pattern standard deviation (PSD) in different glaucoma severity groups

Variable	Subcategory	Glaucoma Severity-OD			p-value
		Early	Moderate	Advanced	
PDS (db)	Mean ± SD	3.68 ± 2.2	6.67 ± 2.15	9.31 ± 2.33	<0.001 *KW
	Median (Min, max)	3.26 (1.38, 9.16)	7.14 (3.59, 9.16)	9.33 (4.58, 12.85)	

PSD values were 3.68 ± 2.2, 6.67 ± 2.15, and 9.31 ± 2.33 for early, moderate, and advanced severity, respectively.

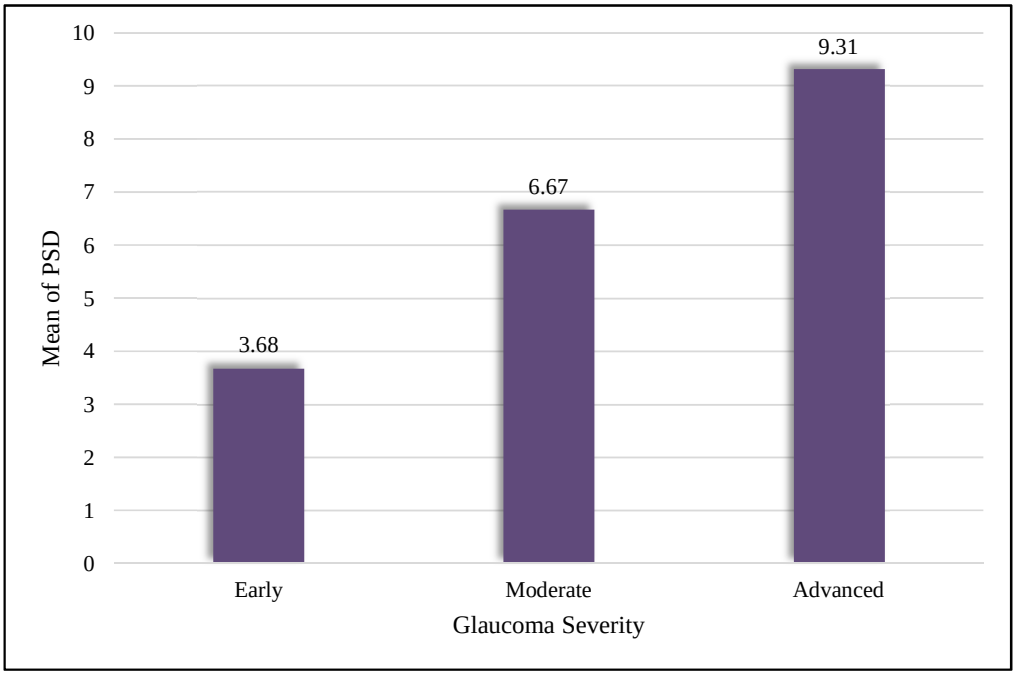

Graph 11: Mean PDS of study participants

The following table shows the total, superior and inferior peripapillary retinal nerve fibre thickness in different glaucoma severity groups.

Table 8. Peripapillary retinal nerve fibre thickness in different glaucoma severity groups

Variable	Subcategory	Glaucoma Severity-OD			p-value
		Early	Moderate	Advanced	
Superior thickness	Mean ± SD Median (Min, max)	118 ± 15 120 (92, 143)	80 ± 24 70 (55, 115)	92 ± 29 92 (42, 136)	<0.001*[A]
Inferior thickness	Mean ± SD Median (Min, max)	124 ± 17 127 (97, 147)	86 ± 26 78 (62, 127)	89 ± 36 93 (24, 134)	<0.001*[A]

The superior retinal nerve fibre cell layer thickness for early, moderate and advanced glaucoma were determined to be 118 ± 15, 80 ± 24 and 92 ± 29, respectively, as mentioned in the above table. The thickness of the inferior retinal nerve fiber layer in early, moderate, and advanced glaucoma was measured as 124 ± 17, 86 ± 26, and 89 ± 36, respectively.

A positive correlation existed linking glaucoma stages and superior and inferior RNFL (p=0.039), indicating minimal RNFL thinning in early glaucoma and substantial thinning occurring as the disease progressed to moderate and advanced stages.

The ganglion cell layer thickness in different glaucoma severity groups has been given in the following table.

Table 9. Ganglion cell layer thickness in different glaucoma severity groups

Variable	Subcategory	Glaucoma Severity-OD			p-value
		Early	Moderate	Advanced	
Ganglion cell layer thickness					
Superior	Mean ± SD Median (Min, max)	62.96 ± 17.09 66 (32, 101)	66.17 ± 16.26 70.5 (42, 84)	56 ± 12.93 59.5 (32, 72)	0.404[A]
Inferior	Mean ± SD Median (Min, max)	65.65 ± 15.18 66 (30, 102)	66.17 ± 17.43 71.5 (39, 84)	56.7 ± 9.81 59.5 (40, 72)	0.109[KW]

The superior ganglion cell layer thickness for early, moderate and advanced glaucoma were determined to be 62.96 ± 17.09, 66.17 ± 16.26 and 56 ± 12.93, respectively, as shown in the table below.

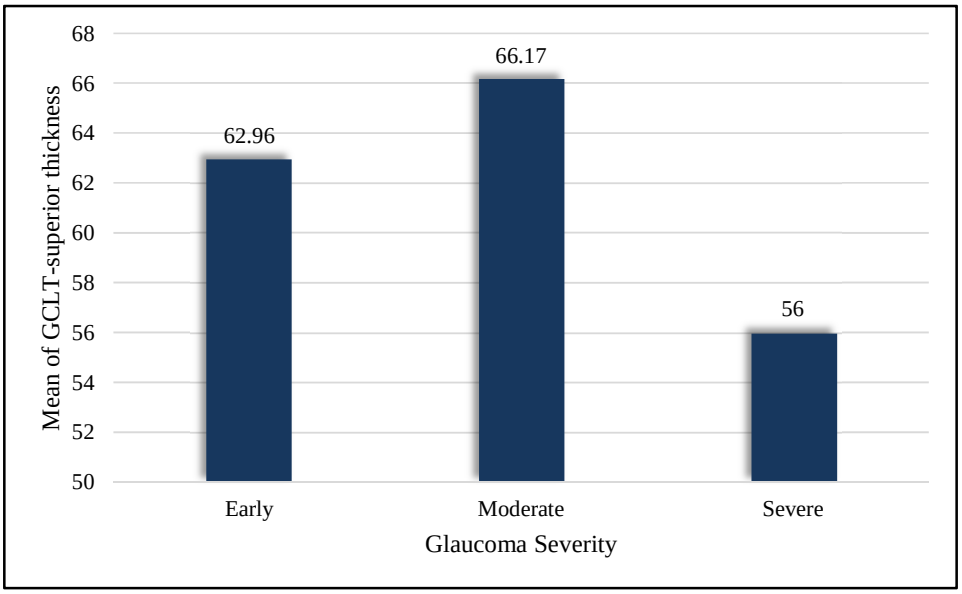

Graph 12: Mean GCL-superior thickness of study participants

The inferior ganglion cell layer thickness for early, moderate and advanced glaucoma were determined to be 65.65 ± 15.18, 66.17 ± 17.43 and 56.7 ± 9.81, respectively, as illustrated in the table below.

There was a significant correlation relating glaucoma stages to ganglion cell layer (GCL)-superior and inferior thickness (p=0.019), indicating that thinning was minimal in early-stage glaucoma; however, significant thinning was noted as the disease progressed.

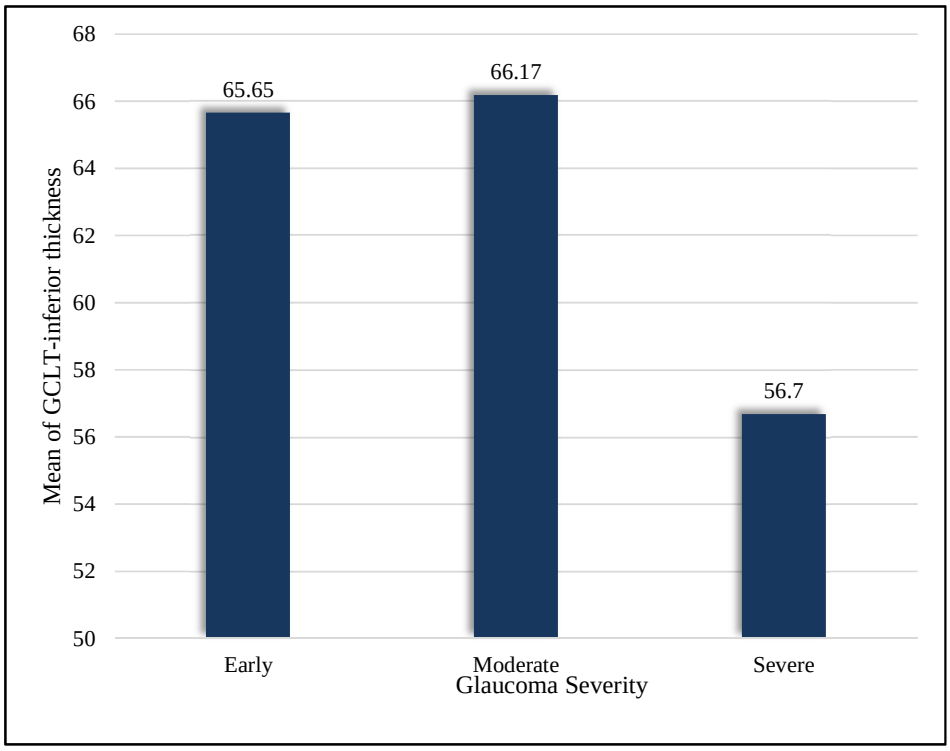

Graph 13: Mean GCL-inferior thickness of study participants

Tukey's Honestly Significant Difference (HSD) test was used for post hoc analysis, and Table 9 provides specifics of the analysis.

Table 10. Post hoc analysis between severity of glaucoma

Variable	Glaucoma severity	p-value
Superior thickness	Early	**0.003**
		0.016
	Moderate	**0.003**
		0.558
	Advanced	**0.016**
		0.558
Inferior thickness	Early	**0.011**
		0.004
	Moderate	**0.011**
		0.983
	Advanced	**0.004**
		0.983

The superior and inferior retinal nerve fiber layer (RNFL) thickness measurements show statistically significant differences ($p < 0.05$) between the early glaucoma group and both the moderate and advanced glaucoma groups.

The correlation between peripapillary RNFL, ganglion cell layer thickness and mean deviation in early, moderate and advanced glaucoma are depicted in the following tables.

Table 11. Correlation between peripapillary RNFL, ganglion cell layer thickness and mean deviation in participants with Early glaucoma

Glaucoma severity			Mean deviation (db)	Superior thickness	Inferior thickness	GCL-Superior	GCL-Inferior
Early	**Mean deviation (db)**	Correlation Coefficient	1.000	-0.475	-0.017	0.128	.334
		p-value	-	0.054	0.95	0.625	0.19
		N	17	17	17	17	17
	Superior thickness	Correlation Coefficient	-0.475	1.000	0.504	-0.098	-0.425
		p-value	0.054	-	**0.039**	0.709	0.089
		N	17	17	17	17	17
	Inferior thickness	Correlation Coefficient	-0.017	0.504	1.000	-0.196	-0.099
		p-value	0.95	**0.039**	-	0.451	0.706
		N	17	17	17	17	17
	GCL-Superior	Correlation Coefficient	0.128	-0.098	-0.196	1.000	0.636
		p-value	0.625	0.709	0.451	-	**0.006**
		N	17	17	17	17	17
	GCL-Inferior	Correlation Coefficient	0.334	-0.425	-0.099	0.636	1.000
		p-value	0.19	0.089	0.706	**0.006**	-

		N	17	17	17	17	17

Table 12. Correlation between peripapillary RNFL, ganglion cell layer thickness and mean deviation in participants with Moderate glaucoma

Moderate	**Mean deviation (db)**	Correlation Coefficient	1.000	-0.116	0.543	-0.086	0.143
		p-value	-	0.827	0.266	0.872	0.787
		N	6	6	6	6	6
	Superior thickness	Correlation Coefficient	-0.116	1.000	0.551	-0.29	-0.58
		p-value	0.827	-	0.257	0.577	0.228
		N	6	6	6	6	6
	Inferior thickness	Correlation Coefficient	0.543	0.551	1.000	0.143	0.086
		p-value	0.266	0.257	-	0.787	0.872
		N	6	6	6	6	6
	GCL-Superior	Correlation Coefficient	-0.086	-0.29	0.143	1.000	0.886
		p-value	0.871	0.577	0.787	-	**0.019**
		N	6	6	6	6	6
	GCL-Inferior	Correlation Coefficient	0.143	-0.58	0.086	0.886	1.000
		p-value	0.787	0.228	0.872	**0.019**	-
		N	6	6	6	6	6

Table 13. Peripapillary RNFL, ganglion cell layer thickness, and mean deviation in individuals with advanced or severe glaucoma are correlated.

Advanced	**Mean deviation (db)**	Correlation Coefficient	1.000	-0.711	-0.83	0.717	0.729
		p-value	-	**0.021**	**0.003**	**0.02**	**0.017**
		N	10	10	10	10	10
	Superior thickness	Correlation Coefficient	-0.711	1.000	0.754	-0.628	-0.534
		p-value	**0.021**	-	**0.012**	0.052	0.112
		N	10	10	10	10	10
	Inferior thickness	Correlation Coefficient	-0.83	0.754	1.000	-0.839	-0.815
		p-value	**0.003**	**0.012**	-	**0.002**	**0.004**
		N	10	10	10	10	10
	GCL-Superior	Correlation Coefficient	0.717	-0.628	-0.839	1.000	0.942
		p-value	**0.02**	0.052	**0.002**	-	**<0.001**
		N	10	10	10	10	10
	GCL-Inferior	Correlation Coefficient	0.729	-0.534	-0.815	0.942	1.000
		p-value	**0.017**	0.112	**0.004**	**<0.001**	-
		N	10	10	10	10	10

Data from the glaucoma severity groups revealed that lower mean deviation scores coincided with thinner superior RNFL (p=0.021) and thinner inferior RNFL (p=0.003) only in advanced cases, however early and moderate cases showed no such

correlation. This implies that there is a progressive loss of RNFL as the mean deviation deteriorates.

A strong positive correlation linked mean deviation to GCL-superior and inferior thickness, with p-values of 0.02 and 0.017, respectively, indicating that worsening mean deviation corresponds to progressive ganglion cell layer thinning.

DISCUSSION

This study was carried out to evaluate RGC damage in patients with POAG by analyzing peripapillary RNFL and macular GCL-IPL thickness using SD-OCT and correlating these findings with visual field changes.

A total of 34 patients were enrolled in the study. The mean age of the study participants was 60.38 ± 12.96 years, indicating that this condition was mostly seen in the elderly. According to E Gramer et al., the average age of patients diagnosed with POAG was 54.81 ± 12.56 years, which aligns with the findings of our study. [80] Similarly, the study conducted by M. Francesca Cordiero et al. revealed that the 70 to 84 years age range constituted the majority of their POAG patient population. [81]

In this study, 28 out of 34 participants were males, demonstrating male predominance in POAG. A study by Vijaya et al. conducted in an urban South Indian population found that 64 out of 135 POAG cases were male, suggesting a slightly higher occurrence in men, comparable to the findings of our study. [82] Similarly, Ramakrishnan et al. examined a rural South Indian population and reported that 37 out of 64 confirmed POAG cases were males. [83]

The most reported comorbidity among the study participants was hypertension (35.10%), followed by diabetes mellitus (21.60%) in this study. Study by Herng-Ching Lin PhD et al. showed that 50.5% of POAG patients presented with hypertension and 30.2% with diabetes, findings which were concordant with our study. [84] Karim Talaat et al. reported that hypertension (60.8%) and diabetes (58.3%) were the most common systemic comorbidities in POAG patients. [85]

The analysis of visual acuity among study participants revealed that 50% had a visual acuity ranging from 6/6 to 6/12, indicating that a significant proportion retained functional vision.

The presence of relative afferent pupillary defect (RAPD) in 2.9% of study participants suggests optic nerve dysfunction.

Assessment of the cup-to-disc (C:D) ratio revealed 58.8% of participants exhibited a C:D ratio between 0.3 to 0.6, whereas 38.2% C:D ratio between 0.7 to 0.9 correlating with the advanced stages of glaucoma in participants. Rao et al., in their study, observed increased cup-to-disc (C:D) ratios in patients (30.3%) presenting with advanced glaucoma, results similar to our study. [86] Likewise, in research by Ramakrishnan et al., conducted in a rural South Indian population, it was observed that individuals with advanced glaucoma had a high cup-to-disc ratio. [83]

The distribution of study participants on glaucoma severity, based on the Hodapp-Parrish-Anderson scale, indicated that 51.5% of participants presented with early glaucoma, while 18.2% were classified as moderate glaucoma and 30.3% had advanced glaucoma. A study by Sharma et al. in North India reported that 48% of subjects presented with early glaucoma, 24% with moderate glaucoma and only a handful of patients, i.e., 28% were diagnosed with advanced stages of glaucoma, results which were consistent with our study. [87] Contrary to the findings of our study, a study done by Seth et al. at a tertiary institute in South India reported that among newly diagnosed glaucoma patients, a significant proportion, i.e., 40% presented with advanced stages of the disease. [88]

The analysis of mean deviation (MD) values across different glaucoma severity groups revealed a worsening of mean deviation as the severity of the disease increased. Patients with early-stage glaucoma had an average MD of -2.87 ± 1.99 dB, which decreased to -9.4 ± 2.06 dB in moderate-stage patients, and further to -15.91 ± 14.24 dB in advanced-stage patients. The Advanced Glaucoma Intervention Study (AGIS) demonstrated a similar trend like our study, where worsening MD values corresponded with disease progression and severity of the disease. [89] Additionally, Yousefi et al. reported that mean deviation (MD) values worsened up to -11 dB, correlating with the advancement of the disease. [90]

The analysis demonstrated a statistically significant increase in Pattern Deviation Scores (PDS) across increasing glaucoma severity levels. Specifically, patients with early-stage glaucoma exhibited a mean PSD of 3.68 ± 2.2, which increased to 6.67 ± 2.15 in moderate-stage and progressed to 9.31 ± 2.33 in advanced-stage glaucoma. The study done by C S Sandhya et al. observed that the PSD values were 5.27 dB for mild, 7.11 dB for moderate, and 10.85 dB for advanced glaucoma, indicating that as glaucoma severity increased, the average PSD values also increased, findings similar to our study. [91] Similarly, Hirasawa et al. emphasized that higher PDS indicates severe glaucomatous damage. [92]

The analysis of superior and inferior retinal nerve fiber layer (RNFL) thicknesses revealed significant differences across severity groups for all three parameters. The superior retinal nerve fibre cell layer thickness for early, moderate and advanced glaucoma were determined to be 118 ± 15, 80 ± 24 and 92 ± 29, respectively. The thickness of the inferior retinal nerve fiber layer in early, moderate, and advanced glaucoma was measured as 124 ± 17, 86 ± 26, and 89 ± 36, respectively. A positive correlation existed linking glaucoma stages and superior and

inferior RNFL (p=0.039), indicating minimal RNFL thinning in early glaucoma, with substantial thinning occurring in advanced stages. Braeu et al. observed structural changes in the optic nerve head, particularly RNFL thinning, that were more pronounced in advanced stages of glaucoma, comparable to our study. [93] Similarly, Vazquez and Huang reported that RNFL analysis via spectral-domain optical coherence tomography provides reliable estimates of glaucomatous optic nerve damage, with greater thinning observed in more severe cases. [94]

The ganglion cell layer (GCL) thickness analysis revealed a progressive decline. While minimal changes were observed in early glaucoma, moderate stages showed a decrease in thickness of both superior and inferior layers, with a further reduction in advanced stages. There was a higher correlation relating glaucoma stages to ganglion cell layer (GCL)-superior and inferior thickness (p=0.019), revealing that thinning was minimal in early glaucoma, however, it became substantially more pronounced in advanced glaucoma. Marie et al. conducted a study to correlate ganglion cell layer thickness with disease severity in patients with POAG and found a significant decline in GCL thickness values with greater glaucoma severity, similar to the finding of our study. [95] Our findings are supported by Acosta et al., who also found a significant correlation (p<0.001) linking average GCL+IPL thickness to moderate glaucoma. [96] In contrast to our findings, Hou et al. reported that the degree of nerve layer thinning (GCL) did not reliably indicate glaucoma severity (p=0.586). [97]

The correlation linking glaucoma stages to retinal nerve fiber layer and ganglion cell layer thickness was stronger for ganglion cell layer thickness (p=0.019) than for retinal nerve fiber layer thickness (p=0.039). This is consistent with the study by Dhabarde et al., where the mean ganglion cell layer thickness for early glaucoma

was lower than that of mean RNFL thickness, indicating superior diagnostic accuracy of GCL thickness in early glaucoma. [98] However, Acosta et al. reported a contrasting result, finding no significant difference between RNFL and GCL layer thickness (p=0.0536) in early glaucoma.[96]

The glaucoma severity groups revealed that lower mean deviation scores coincided with thinner superior RNFL (p=0.021) and thinner inferior RNFL (p=0.003) only in advanced cases, however early and moderate cases showed no such correlation, implying a progressive loss of RNFL as the mean deviation deteriorates. This was consistent with the findings in research by Kim et al., suggesting that deterioration in mean deviation correlates strongly with RNFL thinning (p<0.003). [99] This also aligns with Kanamori et al.'s hypothesis that the average RNFL thickness had the strongest correlation with the mean deviation (p <0.001) [100]

A strong positive correlation linked mean deviation to GCL-superior and inferior thickness, with p-values of 0.02 and 0.017, respectively, indicating that worsening mean deviation corresponds to progressive ganglion cell layer thinning. Similar results were demonstrated in a study by Barua et al., where he found a positive correlation between GCL-superior and GCL-inferior (p<0.01) with mean deviation, emphasizing the interdependence of these parameters. [101] Medeiros et al. reported a high positive correlation between MD and GCL-superior (p=0.02) and GCL-inferior (p=0.017), suggesting that residual GCL integrity influences functional outcomes in late-stage disease. [102]

CONCLUSION

Primary open-angle glaucoma (POAG) is a leading cause of irreversible blindness worldwide, primarily affecting adults. It results in permanent retinal ganglion cell (RGC) loss, accompanied by retinal nerve fibre layer (RNFL) and macular ganglion cell layer-inner plexiform layer (GCL-IPL) degeneration. Early detection and disease monitoring are crucial for preventing vision loss. This research aimed to evaluate RGC damage in POAG patients by analyzing peripapillary RNFL and macular GCL-IPL thickness using SD-OCT and correlating these findings with visual field changes.

The study provides clear evidence of the evolving correlation between retinal structural parameters and functional measures across stages of glaucoma. It underscores the importance of monitoring retinal nerve fiber layer and ganglion cell layer thickness changes to detect glaucoma in its early stages, serving as a sensitive indicator of damage. With glaucoma progression, the correlation between disease severity and ganglion cell layer thickness strengthens, suggesting increasing interdependence. The study revealed that in advanced stages, there is a strong association between visual field deterioration and both retinal nerve fiber layer and ganglion cell layer thinning, demonstrating a strong connection between structural loss and functional decline.

These findings emphasize the importance of comprehensive structural assessment of retinal nerve fibre layer and ganglion cell layer thickness and functional assessment by visual field analysis in glaucoma management, aiding in early detection, monitoring disease progression, and optimizing treatment strategies.

SUMMARY

Primary open-angle glaucoma (POAG) is a leading cause of irreversible blindness worldwide, characterized by progressive retinal ganglion cell (RGC) loss, retinal nerve fiber layer (RNFL) thinning, and visual field (VF) defects. Early detection is crucial for timely intervention. This study evaluates the correlation between peripapillary RNFL and macular ganglion cell-inner plexiform layer (GC-IPL) thickness with VF changes in POAG patients using spectral-domain optical coherence tomography (SD-OCT) and Humphrey Visual Field (HVF) analysis.

A hospital-based observational cross-sectional study was conducted over one year, including 34 POAG patients. RNFL and GC-IPL thicknesses were measured using SD-OCT, and VF analysis was performed with HVF 30-2 SITA Standard. Statistical analysis included correlation assessments between structural and functional parameters.

The results demonstrated significant thinning of RNFL and GC-IPL layers with increasing glaucoma severity. Mean deviation (MD) and pattern standard deviation (PSD) values worsened progressively, with a strong correlation between MD and RNFL thinning in advanced glaucoma ($p=0.003$). GC-IPL thinning showed a significant association with MD across all stages ($p=0.017$), suggesting its potential as an early diagnostic marker. The findings emphasize that GC-IPL thickness is a more sensitive indicator of early glaucomatous damage than RNFL thickness.

This study reinforces the importance of combining structural (RNFL, GC-IPL thickness) and functional (VF analysis) assessments in glaucoma diagnosis and progression monitoring. The use of SD-OCT alongside VF analysis enhances early detection and tracking of disease progression, ultimately contributing to better glaucoma management and vision preservation.

BIBLIOGRAPHY

1. https://webvision.med.utah.edu/book/part-xii-cell-biology-of-retinal-degenerations/what-is-glaucoma/
2. Weinreb RN, Aung T, Medeiros FA. The pathophysiology and treatment of glaucoma: a review. Jama. 2014 May 14;311(18):1901-11.
3. Heijl A, Leske MC, Bengtsson B, Hyman L, Bengtsson B, Hussein M, Early Manifest Glaucoma Trial Group. Reduction of intraocular pressure and glaucoma progression: results from the Early Manifest Glaucoma Trial. Archives of ophthalmology. 2002 Oct 1;120(10):1268-79.
4. Group CN. Comparison of glaucomatous progression between untreated patients with normal-tension glaucoma and patients with therapeutically reduced intraocular pressures. American journal of ophthalmology. 1998 Oct 1;126(4):487-97.
5. Coleman AL, Miglior S. Risk factors for glaucoma onset and progression. Survey of ophthalmology. 2008 Nov 1;53(6):S3-10.
6. Marcus MW, de Vries MM, Montolio FG, Jansonius NM. Myopia as a risk factor for open-angle glaucoma: a systematic review and meta-analysis. Ophthalmology. 2011 Oct 1;118(10):1989-94.
7. Flammer J, Orgül S. Optic nerve blood-flow abnormalities in glaucoma. Progress in retinal and eye research. 1998 Apr 1;17(2):267-89.
8. Resch H, Garhofer G, Fuchsjäger-Mayrl G, Hommer A, Schmetterer L. Endothelial dysfunction in glaucoma. Acta ophthalmologica. 2009 Feb;87(1):4-12.
9. Gharahkhani P, Jorgenson E, Hysi P, Khawaja AP, Pendergrass S, Han X, Ong JS, Hewitt AW, Segrè AV, Rouhana JM, Hamel AR. Genome-wide meta-

analysis identifies 127 open-angle glaucoma loci with consistent effect across ancestries. Nature communications. 2021 Feb 24;12(1):1258.

10. Tham YC, Li X, Wong TY, Quigley HA, Aung T, Cheng CY. Global prevalence of glaucoma and projections of glaucoma burden through 2040: a systematic review and meta-analysis. Ophthalmology. 2014 Nov 1;121(11):2081-90.
11. Mangione CM, Lee PP, Pitts J, Gutierrez P, Berry S, Hays RD, NEI-VFQ Field Test Investigators. Psychometric properties of the National Eye Institute visual function questionnaire (NEI-VFQ). Archives of ophthalmology. 1998 Nov 1;116(11):1496-504.
12. Sotimehin AE, Ramulu PY. Measuring disability in glaucoma. Journal of glaucoma. 2018 Nov 1;27(11):939-49.
13. Schuman JS, Hee MR, Arya AV. Optical coherence tomography. Curr Opin Ophthalmol. 1995;6:89-95.
14. Jaffe GJ, Caprioli J. Optical coherence tomography to detect and manage retinal disease and glaucoma. American journal of ophthalmology. 2004 Jan 1;137(1):156-69.
15. Ang M, Baskaran M, Werkmeister RM, Chua J, Schmidl D, Dos Santos VA, Garhöfer G, Mehta JS, Schmetterer L. Anterior segment optical coherence tomography. Progress in retinal and eye research. 2018 Sep 1;66:132-56.
16. Sigal IA, Wang B, Strouthidis NG, Akagi T, Girard MJ. Recent advances in OCT imaging of the lamina cribrosa. British Journal of Ophthalmology. 2014 Jul 1;98(Suppl 2):ii34-9.
17. Spaide RF, Fujimoto JG, Waheed NK, Sadda SR, Staurenghi G. Optical coherence tomography angiography. Progress in retinal and eye research. 2018 May 1;64:1-55.

18. Takusagawa HL, Liu L, Ma KN, Jia Y, Gao SS, Zhang M, Edmunds B, Parikh M, Tehrani S, Morrison JC, Huang D. Projection-resolved optical coherence tomography angiography of macular retinal circulation in glaucoma. Ophthalmology. 2017 Nov 1;124(11):1589-99.
19. Kolb H. Simple anatomy of the retina.
20. Fortune B. In vivo imaging methods to assess glaucomatous optic neuropathy. Experimental eye research. 2015 Dec 1;141:139-53.
21. Mwanza JC, Oakley JD, Budenz DL, Chang RT, O'Rese JK, Feuer WJ. Macular ganglion cell–inner plexiform layer: automated detection and thickness reproducibility with spectral domain–optical coherence tomography in glaucoma. Investigative ophthalmology & visual science. 2011 Oct 1;52(11):8323-9.
22. Zivkovic M, Dayanir V, Zlatanovic M, Zlatanovic G, Jaksic V, Jovanovic P, Radenkovic M, Djordjevic-Jocic J, Stankovic-Babic G, Jovanovic S. Ganglion cell-inner plexiform layer thickness in different glaucoma stages measured by optical coherence tomography. Ophthalmic research. 2018 Apr 12;59(3):148-54.
23. Hood DC. Improving our understanding, and detection, of glaucomatous damage: an approach based upon optical coherence tomography (OCT). Progress in retinal and eye research. 2017 Mar 1;57:46-75.
24. Mwanza JC, Durbin MK, Budenz DL, Sayyad FE, Chang RT, Neelakantan A, Godfrey DG, Carter R, Crandall AS. Glaucoma diagnostic accuracy of ganglion cell–inner plexiform layer thickness: comparison with nerve fiber layer and optic nerve head. Ophthalmology. 2012 Jun 1;119(6):1151-8.

25. Lee WJ, Oh S, Kim YK, Jeoung JW, Park KH. Comparison of glaucoma-diagnostic ability between wide-field swept-source OCT retinal nerve fiber layer maps and spectral-domain OCT. Eye. 2018 Sep;32(9):1483-92.
26. Kur J, Newman EA, Chan-Ling T. Cellular and physiological mechanisms underlying blood flow regulation in the retina and choroid in health and disease. Progress in retinal and eye research. 2012 Sep 1;31(5):377-406.
27. Henkind P. Radial peripapillary capillaries of the retina. I. Anatomy: human and comparative. The British journal of ophthalmology. 1967 Feb;51(2):115.
28. An D, Yu P, Freund KB, Yu DY, Balaratnasingam C. Three-dimensional characterization of the normal human parafoveal microvasculature using structural criteria and high-resolution confocal microscopy. Investigative ophthalmology & visual science. 2020 Aug 3;61(10):3-.
29. Cabral D, Fradinho AC, Pereira T, Ramakrishnan MS, Bacci T, An D, Tenreiro S, Seabra MC, Balaratnasingam C, Freund KB. Macular vascular imaging and connectivity analysis using high-resolution optical coherence tomography. Translational vision science & technology. 2022 Jun 1;11(6):2-.
30. Delaey C, Van de Voorde J. Regulatory mechanisms in the retinal and choroidal circulation. Ophthalmic research. 2000 Oct 17;32(6):249-56.
31. Hayreh SS. Segmental nature of the choroidal vasculature. British Journal of Ophthalmology. 1975 Nov 1;59(11):631-48.
32. Hayreh SS. Blood supply of the optic nerve head and its role in optic atrophy, glaucoma, and oedema of the optic disc. The British journal of ophthalmology. 1969 Nov;53(11):721.
33. Olver JM, Spalton DJ, McCartney AC. Quantitative morphology of human retrolaminar optic nerve vasculature. Investigative ophthalmology & visual science. 1994 Oct 1;35(11):3858-66.

34. Newman EA. Functional hyperemia and mechanisms of neurovascular coupling in the retinal vasculature. Journal of Cerebral Blood Flow & Metabolism. 2013 Nov;33(11):1685-95.

35. Drexler W, Morgner U, Ghanta RK, Kärtner FX, Schuman JS, Fujimoto JG. Ultrahigh-resolution ophthalmic optical coherence tomography. Nature medicine. 2001 Apr;7(4):502-7.

36. Budenz DL, Michael A, Chang RT, McSoley J, Katz J. Sensitivity and specificity of the StratusOCT for perimetric glaucoma. Ophthalmology. 2005 Jan 1;112(1):3-9.

37. Wojtkowski M, Srinivasan VJ, Ko TH, Fujimoto JG, Kowalczyk A, Duker JS. Ultrahigh-resolution, high-speed, Fourier domain optical coherence tomography and methods for dispersion compensation. Optics express. 2004 May 31;12(11):2404-22.

38. Liu B, Brezinski ME. Theoretical and practical considerations on detection performance of time domain, Fourier domain, and swept source optical coherence tomography. Journal of biomedical optics. 2007 Jul 13;12(4):044007-

39. Lains I, Wang JC, Cui Y, Katz R, Vingopoulos F, Staurenghi G, Vavvas DG, Miller JW, Miller JB. Retinal applications of swept source optical coherence tomography (OCT) and optical coherence tomography angiography (OCTA). Progress in retinal and eye research. 2021 Sep 1;84:100951.

40. Lisboa R, Leite MT, Zangwill LM, Tafreshi A, Weinreb RN, Medeiros FA. Diagnosing preperimetric glaucoma with spectral domain optical coherence tomography. Ophthalmology. 2012 Nov 1;119(11):2261-9.

41. Mwanza JC, Durbin MK, Budenz DL, Sayyad FE, Chang RT, Neelakantan A, Godfrey DG, Carter R, Crandall AS. Glaucoma diagnostic accuracy of ganglion

cell–inner plexiform layer thickness: comparison with nerve fiber layer and optic nerve head. Ophthalmology. 2012 Jun 1;119(6):1151-8.

42. Rao HL, Kumbar T, Addepalli UK, Bharti N, Senthil S, Choudhari NS, Garudadri CS. Effect of spectrum bias on the diagnostic accuracy of spectral-domain optical coherence tomography in glaucoma. Investigative Ophthalmology & Visual Science. 2012 Feb 1;53(2):1058-65.
43. Kuang TM, Zhang C, Zangwill LM, Weinreb RN, Medeiros FA. Estimating lead time gained by optical coherence tomography in detecting glaucoma before development of visual field defects. Ophthalmology. 2015 Oct 1;122(10):2002-9.
44. Jeoung JW, Park KH. Comparison of Cirrus OCT and Stratus OCT on the ability to detect localized retinal nerve fiber layer defects in preperimetric glaucoma. Investigative ophthalmology & visual science. 2010 Feb 1;51(2):938-45.
45. Cheng L, Wang M, Deng J, Lv M, Jiang W, Xiong S, Sun S, Zhu J, Zou H, He X, Xu X. Macular ganglion cell-inner plexiform layer, ganglion cell complex, and outer retinal layer thicknesses in a large cohort of Chinese children. Investigative ophthalmology & visual science. 2019 Nov 1;60(14):4792-802.
46. Singh S, Dass R. The central artery of the retina II. A study of its distribution and anastomoses. The British Journal of Ophthalmology. 1960 May;44(5):280.
47. Sung KR, Wollstein G, Kim NR, Na JH, Nevins JE, Kim CY, Schuman JS. Macular assessment using optical coherence tomography for glaucoma diagnosis. British journal of ophthalmology. 2012 Dec 1;96(12):1452-5.
48. Yang Z, Tatham AJ, Weinreb RN, Medeiros FA, Liu T, Zangwill LM. Diagnostic ability of macular ganglion cell inner plexiform layer measurements

in glaucoma using swept source and spectral domain optical coherence tomography. PLoS One. 2015 May 15;10(5):e0125957.

49. Seol BR, Jeoung JW, Park KH. Glaucoma detection ability of macular ganglion cell-inner plexiform layer thickness in myopic preperimetric glaucoma. Investigative ophthalmology & visual science. 2015 Dec 1;56(13):8306-13.

50. Nakanishi H, Akagi T, Hangai M, Kimura Y, Suda K, Kumagai KK, Morooka S, Ikeda HO, Yoshimura N. Sensitivity and specificity for detecting early glaucoma in eyes with high myopia from normative database of macular ganglion cell complex thickness obtained from normal non-myopic or highly myopic Asian eyes. Graefe's Archive for Clinical and Experimental Ophthalmology. 2015 Jul;253:1143-52.

51. Lee WJ, Oh S, Kim YK, Jeoung JW, Park KH. Comparison of glaucoma-diagnostic ability between wide-field swept-source OCT retinal nerve fiber layer maps and spectral-domain OCT. Eye. 2018 Sep;32(9):1483-92.

52. Chauhan BC, O'Leary N, AlMobarak FA, Reis AS, Yang H, Sharpe GP, Hutchison DM, Nicolela MT, Burgoyne CF. Enhanced detection of open-angle glaucoma with an anatomically accurate optical coherence tomography–derived neuroretinal rim parameter. Ophthalmology. 2013 Mar 1;120(3):535-43.

53. Kim YW, Park KH. Diagnostic accuracy of three-dimensional neuroretinal rim thickness for differentiation of myopic glaucoma from myopia. Investigative ophthalmology & visual science. 2018 Jul 2;59(8):3655-66.

54. Mwanza JC, Warren JL, Budenz DL. Utility of combining spectral domain optical coherence tomography structural parameters for the diagnosis of early Glaucoma: a mini-review. Eye and vision. 2018 Dec;5:1-1.

55. Wu Z, Medeiros FA. Comparison of visual field point-wise event-based and global trend-based analysis for detecting glaucomatous progression. Translational vision science & technology. 2018 Jul 1;7(4):20-.

56. Medeiros FA, Leite MT, Zangwill LM, Weinreb RN. Combining structural and functional measurements to improve detection of glaucoma progression using Bayesian hierarchical models. Investigative ophthalmology & visual science. 2011 Jul 1;52(8):5794-803.

57. Kim KE, Yoo BW, Jeoung JW, Park KH. Long-term reproducibility of macular ganglion cell analysis in clinically stable glaucoma patients. Investigative ophthalmology & visual science. 2015 Jul 1;56(8):4857-64.

58. Mwanza JC, Budenz DL, Warren JL, Webel AD, Reynolds CE, Barbosa DT, Lin S. Retinal nerve fibre layer thickness floor and corresponding functional loss in glaucoma. British Journal of Ophthalmology. 2015 Jun 1;99(6):732-7.

59. Mwanza JC, Kim HY, Budenz DL, Warren JL, Margolis M, Lawrence SD, Jani PD, Thompson GS, Lee RK. Residual and dynamic range of retinal nerve fiber layer thickness in glaucoma: comparison of three OCT platforms. Investigative ophthalmology & visual science. 2015 Oct 1;56(11):6344-51.

60. Shin JW, Sung KR, Lee GC, Durbin MK, Cheng D. Ganglion cell–inner plexiform layer change detected by optical coherence tomography indicates progression in advanced glaucoma. Ophthalmology. 2017 Oct 1;124(10):1466-74.

61. Sung KR, Sun JH, Na JH, Lee JY, Lee Y. Progression detection capability of macular thickness in advanced glaucomatous eyes. Ophthalmology. 2012 Feb 1;119(2):308-13.

62. Lee WJ, Kim YK, Park KH, Jeoung JW. Trend-based analysis of ganglion cell–inner plexiform layer thickness changes on optical coherence tomography in glaucoma progression. Ophthalmology. 2017 Sep 1;124(9):1383-91.

63. Kim YK, Ha A, Na KI, Kim HJ, Jeoung JW, Park KH. Temporal relation between macular ganglion cell–inner plexiform layer loss and peripapillary retinal nerve fiber layer loss in glaucoma. Ophthalmology. 2017 Jul 1;124(7):1056-64.

64. Hou HW, Lin C, Leung CK. Integrating macular ganglion cell inner plexiform layer and parapapillary retinal nerve fiber layer measurements to detect glaucoma progression. Ophthalmology. 2018 Jun 1;125(6):822-31.

65. Lee WJ, Kim TJ, Kim YK, Jeoung JW, Park KH. Serial combined wide-field optical coherence tomography maps for detection of early glaucomatous structural progression. JAMA ophthalmology. 2018 Oct 1;136(10):1121-7.

66. Hood DC, Tsamis E, Bommakanti NK, Joiner DB, Al-Aswad LA, Blumberg DM, Cioffi GA, Liebmann JM, De Moraes CG. Structure-function agreement is better than commonly thought in eyes with early glaucoma. Investigative ophthalmology & visual science. 2019 Oct 1;60(13):4241-8.

67. Hood DC, Xin D, Wang D, Jarukasetphon R, Ramachandran R, Grillo LM, De Moraes CG, Ritch R. A region-of-interest approach for detecting progression of glaucomatous damage with optical coherence tomography. JAMA ophthalmology. 2015 Dec 1;133(12):1438-44.

68. Vianna JR, Malik R, Danthurebandara VM, Sharpe GP, Belliveau AC, Shuba LM, Chauhan BC, Nicolela MT. Beta and gamma peripapillary atrophy in myopic eyes with and without glaucoma. Investigative ophthalmology & visual science. 2016 Jun 1;57(7):3103-11.

69. Abd El-Naby AE, Abouelkheir HY, Al-Sharkawy HT, Mokbel TH. Correlation of retinal nerve fiber layer thickness and perimetric changes in primary open-angle glaucoma. Journal of the Egyptian Ophthalmological Society. 2018 Jan 1;111(1):7-14.

70. Hou HW, Lin C, Leung CK. Integrating macular ganglion cell inner plexiform layer and parapapillary retinal nerve fiber layer measurements to detect glaucoma progression. Ophthalmology. 2018 Jun 1;125(6):822-31.

71. Lin PW, Chang HW, Lin JP, Lai C. Analysis of peripapillary retinal nerve fiber layer and inner macular layers by spectral-domain optical coherence tomography for detection of early glaucoma. International Journal of Ophthalmology. 2018;11(7):1163.

72. Deshpande G, Gupta R, Bawankule P, Raje D, Chakarborty M. Structural evaluation of preperimetric and perimetric glaucoma. Indian journal of ophthalmology. 2019 Nov 1;67(11):1843-9.

73. Ustaoglu M, Solmaz N, Onder F. Discriminating performance of macular ganglion cell-inner plexiform layer thicknesses at different stages of glaucoma. International Journal of Ophthalmology. 2019;12(3):464.

74. Xu XY, Lai KB, Xiao H, Lin YQ, Guo XX, Liu X. Comparisons of ganglion cell-inner plexiform layer loss patterns and its diagnostic performance between normal tension glaucoma and primary open angle glaucoma: a detailed, severity-based study. International Journal of Ophthalmology. 2020;13(1):71.

75. Gupta P, Minj A, Das S, Panigrahi PK. To Compare and Correlate Visual Field Changes Detected by Perimetry with Retinal Nerve Fiber Layer and Ganglion Cell Layer Thickness Observed Using Spectral Domain Optical Coherence Tomography in Primary Open Angle Glaucoma. TNOA Journal of Ophthalmic Science and Research. 2021 Oct 1;59(4):344-9.

76. Bhat KS, Reddy MV, Pai V. Correlation of retinal nerve fiber layer thickness with perimetric staging in primary open-angle glaucoma–A cross-sectional study. Oman Journal of Ophthalmology. 2022 Jan 1;15(1):36-42.

77. Rabiolo A, Fantaguzzi F, Montesano G, Brambati M, Sacconi R, Gelormini F, Triolo G, Bettin P, Querques G, Bandello F. Comparison of Retinal Nerve Fiber Layer and Ganglion Cell–Inner Plexiform Layer Thickness Values Using Spectral-Domain and Swept-Source OCT. Translational Vision Science & Technology. 2022 Jun 1;11(6):27-.

78. Luttrull JK, Tzekov R, Bhavan SV. Progressive Thickening of Retinal Nerve Fiber and Ganglion Cell Complex Layers Following SDM Laser Vision Protection Therapy in Open-Angle Glaucoma. Ophthalmology and Therapy. 2024 Sep 19:1-6.

79. San Pedro MJ, Sosuan GM, Yap-Veloso MI. Correlation of Macular Ganglion Cell Layer+ Inner Plexiform Layer (GCL+ IPL) and Circumpapillary Retinal Nerve Fiber Layer (cRNFL) Thickness in Glaucoma Suspects and Glaucomatous Eyes. Clinical Ophthalmology. 2024 Dec 31:2313-25.

80. E Gramer, G Gramer; Age of the Patients at the Time of Diagnosis in Different Glaucomas: A Prospective Study. Invest. Ophthalmol. Vis. Sci. 2002;43(13):3422

81. Cordeiro, M. F., Denis, P., Astarita, C., Belsey, J., Rivas, M., & García-Feijoo, J. (2024). Prevalence of comorbidities with the potential to increase the risk of nonadherence to topical ocular hypotensive medication in patients with open-angle glaucoma. Current Medical Research and Opinion, 40(4), 647–655. https://doi.org/10.1080/03007995.2024.2322048

82. Vijaya L, George R, Baskaran M, Arvind H, Raju P, Ramesh SV, et al. Prevalence of primary open-angle glaucoma in an urban south Indian population

and comparison with a rural population. The Chennai Glaucoma Study. Ophthalmology. 2008 Apr;115(4):648-654.e1.

83. R , Pk N, R K, Rd T, Jm T, J K, et al. Glaucoma in a rural population of southern India: the Aravind comprehensive eye survey. Ophthalmology [Internet]. 2003 Aug [cited 2025 Mar 2];110(8). Available from: https://pubmed.ncbi.nlm.nih.gov/12917161/

84. Herng-Ching Lin, Ching-Wen Chien, Chao-Chien Hu, Jau-Der Ho, Comparison of Comorbid Conditions between Open-Angle Glaucoma Patients and a Control Cohort: A Cas e-Control Study, Ophthalmology, Volume 117, Issue 11, 2010, Pages 2088-2095, ISSN 0161-6420

    Talaat K, Fathi OT, Alamoudi SM, Alzahrani MG, Mukhtar RM, Khan MA. Types of Glaucoma and Associated Comorbidities Among Patients at King Abdulaziz Medical City, Jeddah. Cureus. 2021 Jun 10;13(6):e15574. doi: 10.7759/cureus.15574. PMID: 34277196; PMCID: PMC8270073.

85. Rao HL, Pradhan ZS, Weinreb RN, Riyazuddin M, Dasari S, Venugopal JP, et al. A comparison of the diagnostic ability of vessel density and structural measurements of optical coherence tomography in primary open angle glaucoma. PLOS ONE. 2017 Mar 13;12(3):e0173930.

86. Research (IJHSR) IJ of HS and. Profile and Clinical Characteristics of Newly Diagnosed Glaucoma in Tertiary Eye Hospital in North India. International Journal of Health Sciences and Research [Internet]. 2024 [cited 2025 Mar 2];14(12). Available from: https://www.ijhsr.org/IJHSR_Vol.14_Issue.12_Dec2024/IJHSR-Abstract15.html

87. Seth PK, Senthil S, Das AV, Garudadri C. Prevalence of glaucoma types, clinical profile and disease severity at presentation: Tertiary Institute based

cross-sectional study from South India. Indian J Ophthalmol. 2023 Oct;71(10):3305–12.

88. The Advanced Glaucoma Intervention Study (AGIS): 14. Distinguishing progression of glaucoma from visual field fluctuations. Ophthalmology. 2004 Nov 1;111(11):2109-2116.e4.
89. Yousefi S, Nezhad GSM, Pourahmad S, Vermeer KA, Lemij HG. Distribution and Rates of Visual Field Loss across Different Disease Stages in Primary Open-Angle Glaucoma. Ophthalmology Glaucoma. 2018 Jul 1;1(1):52–60.
90. Sandhya CS, Nookala GP, Karimoon T, Harris T. Comparison of visual fields and retinal nerve fiber layer thickness in assessing optic nerve head damage in patients with primary open-angle glaucoma. Indian J Clin Exp Ophthalmol. 2022;8(2):210. doi:10.18231/j.ijceo.2022.042.
91. K H, N S, T M, K S. A modified glaucoma staging system based on visual field index. Graefe's archive for clinical and experimental ophthalmology = Albrecht von Graefes Archiv fur klinische und experimentelle Ophthalmologie [Internet]. 2013 Dec [cited 2025 Mar 2];251(12). Available from: https://pubmed.ncbi.nlm.nih.gov/24136631/
92. Fabian A. Braeu, Thanadet Chuangsuwanich, Tin A. Tun, Shamira A. Perera, Rahat Husain, Aiste Kadziauskiene, Leopold Schmetterer, Alexandre H. Thiéry, George Barbastathis, Tin Aung, Michaël J.A. Girard. The 3D Structural Phenotype of the Glaucomatous Optic Nerve Head and its Relationship with The Severity of Visual Field Damage. arxiv.
93. https://fyra.io. RNFL Analysis in the Diagnosis of Glaucoma [Internet]. Glaucoma Today. Bryn Mawr Communications; [cited 2025 Mar 2]. Available from: https://glaucomatoday.com/articles/2016-may-june/rnfl-analysis-in-the-diagnosis-of-glaucoma

94. https://www.dovepress.com/correlation-of-macular-ganglion-cell-layer--inner-plexiform-layer-gcl--peer-reviewed-fulltext-article-OPTH

95. Acosta, Patricia Camille O; de Leon, John Mark S. Correlation of peripapillary retinal nerve fiber layer and macular ganglion cell–inner plexiform layer in early to moderate glaucoma using the Cirrus® widefield analysis (PanoMap®). Indian Journal of Ophthalmology 72(3):p 412-416, March 2024. | DOI: 10.4103/IJO.IJO_697_23

96. Hou JH, Zhu HX, Zhou ML, Le WB, Zeng CH, Liang SS, et al. Changes in the Spectrum of Kidney Diseases: An Analysis of 40,759 Biopsy-Proven Cases from 2003 to 2014 in China. KDD. 2018;4(1):10–9.

97. Dhabarde, Kavita A; Kende, Rohit P; Rahul, Nisha V; Surabhi, ; Nangare, Aditi R. Structure–function relationship and diagnostic value of macular ganglion cell complex measurement using Fourier-domain OCT in glaucoma. Indian Journal of Ophthalmology 72(3):p 363-369, March 2024. | DOI: 10.4103/IJO.IJO_771_23

98. Kim HJ, Sung MS, Park SW. Factors Associated with Visual Acuity in Advanced Glaucoma. J Clin Med. 2023 Apr 24;12(9):3076. doi: 10.3390/jcm12093076. PMID: 37176517; PMCID: PMC10179664.

99. Kanamori A, Nakamura M, Escano MFT, Seya R, Maeda H, Negi A. Evaluation of the glaucomatous damage on retinal nerve fiber layer thickness measured by optical coherence tomography. Am J Ophthalmol. 2003 Apr;135(4):513–20.

100. Barua N, Sitaraman C, Goel S, Chakraborti C, Mukherjee S, Parashar H. Comparison of diagnostic capability of macular ganglion cell complex and retinal nerve fiber layer among primary open angle glaucoma, ocular hypertension, and normal population using Fourier-domain optical coherence

tomography and determining their functional correlation in Indian population. Indian J Ophthalmol. 2016 Apr 1;64(4):296–302.

101. Medeiros FA, Jammal AA. Validation of Rates of Mean Deviation Change as Clinically Relevant End Points for Glaucoma Progression. Ophthalmology. 2023 May;130(5):469–77

ANNEXURES

ANNEXURE – I - INFORMED CONSENT FORM

"To correlate peripapillary retinal nerve fibre layer thickness and macular ganglion cell layer- inner plexiform layer thickness with visual field changes in patients of primary open angle glaucoma by spectral domain optical coherence tomography"

- Name of Student/Principal Investigator:
- Name of Guide/Co Investigators:

Introduction: Primary open angle glaucoma is a chronic progressive optic neuropathy characterised by retinal cell death and associated visual field loss. It is one of the leading causes of irreversible blindness in the world. Therefore, it is very important to diagnose and treat glaucoma at early stages, in order to prevent permanent damage. Measuring peripapillary retinal nerve fiber thickness by spectral domain optical tomography can aid in diagnosing primary open angle glaucoma in pre-perimetric stages and assess the progression of disease, which can further help in changing treatment modalities accordingly.

Explanation of procedure: The study involves patients to undergo investigation of spectral domain optical coherence tomography for the measurement of peripapillary retinal nerve fiber and macular ganglion cell layer thickness. The patient will also undergo series of investigations like measurement of intra ocular pressure by non-contact tonometry, applanation tonometry, disc evaluation by indirect ophthalmoscope and measurement of anterior chamber angle by gonioscopy to predict the prognosis of the disease.

Withdrawal from participation in the study: Participation in this study in voluntary.

You will be free to decide whether to participate in this study or continue participation once enrolled. In case you decide to withdraw your participation, you are free to do so. However, please convey the decision to the principal investigator.

Possible benefits from participating in the study: The study will benefit the patients by helping them recognise and understand the prognosis of their disease. The data gathered will help population at large as the study will help analysing the severity of primary open angle glaucoma.

Possible risks from participating in the study: There are no risks involved in participating in this study.

Privacy and confidentiality: The information collected from you will be coded, to prevent any person to identify you. Your identity will never be revealed. The data collected from you will be kept confidential and only processed or aggregated data will be used for publication.

Financial incentives: You will not receive any payment for participating in this study.

Cost of investigations done during the course of study will be paid by the Participant.

Authorization for publication of aggregated data: Results obtained after processing of the aggregated data will be published for scientific purpose and or presented to scientific groups.

However, your identity will never be revealed.

Questions: In case of any questions with regard to this study, you are free to contact: "7999170799" If you have any question or complaints with regard to your right as study participant you may contact Dr Harsha Hegde, Chairperson, Ethical committee of JNMC, 0831-2473777 Extension 4052.

Legal rights: By signing this consent form, we are not waving any of your legal rights

CONSENT STATEMENT

I am making a voluntary decision to participate in the study "To correlate peripapillary retinal nerve fibre layer thickness and macular ganglion cell layer- inner plexiform layer thickness with visual field changes in patients of primary open angle glaucoma by spectral domain optical coherence tomography." My signature below indicates that I have decided to participate and I have read the information provided above or the information provided above has been read to me in the language that I understand best. I was given the opportunity to ask questions and that they have been answered to my satisfaction.

Name of the participant:

Signature or left thumb impression of the participant: Name of the witness:

Signature or left thumb impression of the witness: Name of the investigator:

Signature of the investigator: Date of investigation:

ANNEXURE II PROFORMA

GENERAL INFORMATION

PATIENT ID NUMBER:

NAME: _____

AGE:_____GENDER: F/M_____CONTACT NUMBER:_____

ADDRESS: _____

Has informed consent

been given? YES/NOInformant – self

CHIEF COMPLAINTS: -

HISTORY OF PRESENTING ILLNESS

PAST HISTORY

Ocular surgery: Yes/No

Type of Surgery: _____ Duration: days/months/years

Ocular trauma: Yes/No

MEDICAL HISTORY

Systemic illness if any

FAMILY HISTORY

Similar complaints in any of the family member (1st degree relative)

	OD	OS
DISTANT		
NEAR		
PINHOLE		
AIDED		

SUBJECTIVE CORRECTION:

	RE	SPH	CYL	AXIS	SPH	CYL	AXIS	LE
DIST.VN								

ANTERIOR SEGMENT EXAMINATION:

	OD	OS
LIDS		
CONJUNCTIVA		
CORNEA		
ANTERIOR CHAMBER		
IRIS		
PUPIL		
LENS		

FUNDUS FINDINGS:

	OD	OS
GLOW		
MEDIA		
DISC		
C:D RATIO		
BLOOD VESSELS		
BACKGROUND		
MACULA		

DISC PARAMETERS:

	OD	OS
Disc diameter		
Cup diameter		
Neuroretinal rim (shape and pallor)		
Cup:Disc ratios		
Cup:Disc area		
Presence of splinter hemorrhages		
Lamellar dot sign		
Bayonetting sign		
Presence of Notching		
Peripapillary atrophy		

IOP-

By noncontact tonometry

RE-mm hg

LE- mm hg

By applanation tonometry

OD mm hg

OS mm hg

Gonioscopy: OD OS

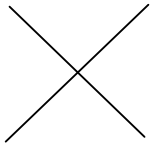

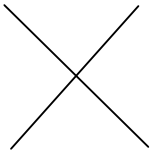

PERIMETRY:

	OD	OS
Mean deviation		
Glaucoma severity		
Pattern standard deviation		
Fixation losses		
False positives		
False negatives		

OPTICAL COHERENCE TOMOGRAPHY:

	OD	OS
AVERAGE RNFL THICKNESS		
a) Total thickness		
b) Superior thickness		
c) Inferior thickness		
DISC AREA		
CUP AREA		
CUP DISC RATIO		
GANGLION CELL LAYER THICKNESS		
SUPERIOR		
INFERIOR		

NAME OF INVESTIGATOR:

SIGNATURE:

NAME OF GUIDE:

SIGNATURE:

ANNEXURE III: PHOTOGRAPHS

Photograph 1: Assessment of optic nerve head with 90D and slit lamp biomicroscopy

Photograph 2: Measurement of IOP by Applanation Tonometry

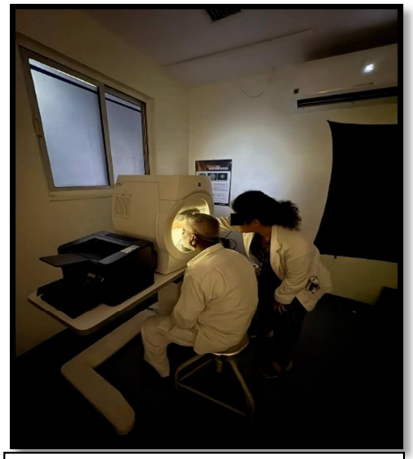

Photograph 3: Visual field analysis with Humphery's field analyser

Photograph 4: RNFL and GCL analysis with spectral domain OCT

ANNEXURE IV: MASTER CHART

sl no	Name	Age	Sex	Family history	RE Visual acuity	RE BCVA	DM/HTN	Anterior segment OD	Fundus OD	Presence of splinter hemorrhages, lamellar dot sign, bayonetting sign presence of notching, PPA	IOP by NCT (RE)	IOP by AT (RE)	Gonioscopy (RE,LE)	Type of perimetry	Mean deviation OD	PSD OD	Glaucoma severity OD	Total thickness OD	Superior thickness OD	Inferior thickness OD	Disc area OD	Cup area OD	Cup disc ratio OD	Rim area OD	Ganglion cell layer thickness OD
1	**Kallappa Virupaxappa Badiger**	55	male	nil	6/6	6/6	HTN	WNL	C:D 0.4	NIL	31.2	28	OD: OPEN, OS: OPEN	30-2 SITA STD	-6.15db	1.47db	early	85	108	106	1.95	1.07	0.55	0.88	S: 61, I: 61
2	**Althab Rajasab Sanadi**	48	male	nil	6/18	6/9(p)	HTN	WNL	C:D 0.7	NIL	21.1	22	OD: OPEN, OS: OPEN	30-2 SITA STD	-13.18db	12.85db	advanced	75	96	92	2.24	1.6	0.71	0.64	S: 57, I: 50
3	**Hasansab Baddesab Sanadi**	76	male	nil	6/18(p)	6/12	HTN	WNL	C:D 0.6	OU nasalisation, bayonetting, thinning	25.4	28	OD: OPEN, OS: OPEN	30-2 SITA STD	-1.25db	3.26	early	88	92	97	2.42	1.65	0.68	0.68	S: 62, I: 61
4	**Dastageer Runddas Mokashi**	75	male	nil	6/18(p)	6/12	nil	WNL	C:D 0.7	NIL	11.7	22	OD: OPEN, OS: OPEN	30-2 SITA STD	-21.39db	9.3	advanced	82	84	115	2.73	1.15	0.75	0.63	S: 40, I: 54
5	**Rajaraaam Dawalat Padwaal**	84	male	nil	6/36	6/12	nil	WNL	C:D 0.6	OD: splinter hemorrhages at disc margin	25.8	26	OD: OPEN, OS: OPEN	30-2 SITA STD	-11.56db	8.27	moderate	61	68	66	2.13	1.48	0.69	0.65	S: 32, I: 40
6	**Shamsundar Virupaxi**	73	male	nil	6/12(p)	6/6(p)	HTN,IHD	WNL	C:D 0.5	OD: laminar dot sign, bayonetting, thinning	14.5	16	OD: OPEN, OS: OPEN	30-2 SITA STD	-20.69db	11.32	advanced	88	117	79	1.86	1.76	0.69	0.86	S: 46, I: 44
7	**Sandhya Irappa Gadadavar**	51	female	nil	6/24	6/9(p)	nil	WNL	C:D 0.4	NIL	15.5	18	OD: OPEN, OS: OPEN	30-2 SITA STD	-1.20db	1.78	early	89	106	107	2.67	1.12	0.42	1.62	S: 61, I: 60
8	**Murlidhar Shrinivar Kanekar**	68	male	nil	6/60	6/12	nil	WNL	C:D 0.6	OU: PPA	23.1	20	OD: OPEN, OS: OPEN	30-2 SITA STD	-7.80db	3.59	moderate	102	115	127	3.11	1.25	0.5	1.86	S: 72, I: 66
9	**Sambhaji Vikrant Bhosale**	48	male	nil	6/12(p)	6/6	nil	WNL	C:D 0.4, drussens in periphery	NIL	18.7	20	OD: OPEN, OS: OPEN	30-2 SITA STD	-0.85db	9.39	early	87	104	107	2.62	1.14	0.47	1.09	S: 71, I: 72
10	**Savita S Patil**	54	female	nil	6/9(p)	6/6	HTN	WNL	C:D 0.6	NIL	24.4	22	OD: OPEN, OS: OPEN	30-2 SITA STD	-30.18db	4.58	advanced	105	136	134	2.52	1.72	0.71	0.74	S: 58, I: 59
11	**Sanjay Kagatikar**	52	male	nil	6/6	6/6	nil	WNL	C:D 0.7	NIL	11.7	14	OD: OPEN, OS: OPEN	30-2 SITA STD	-1.63db	2.44	early	109	125	143	3.02	1.98	0.65	1.04	S: 101, I: 102

12	**Suhas Shivanand Khanpat**	33	male	nil	6/12	6/6(p)	Type I DM	Few cortical opacities	C:D 0.5	OU: presence of notching	18.6	16	OD: OPEN, OS: OPEN	30-2 SITA STD	-1.63db	2.44	early	99	120	127	2.75	1.86	0.88	0.88	S: 66, I: 64
13	**Ramkrishna Ramchandra Talwar**	78	male	nil	6/36	6/12	nil	WNL	C:D 0.8	OS: thinning of NRR	20.6	18	OD: OPEN, OS: OPEN	30-2 SITA STD	-6.02db	6.11	early	100	122	136	2.11	1.47	0.7	0.64	S: 84, I: 79
14	**Ranjita Shrikant Sankangoudar**	36	female	nil	6/9	6/6	nil	WNL	C:D 0.6	NIL	30.2	28	OD: OPEN, OS: OPEN	30-2 SITA STD	-23.64db	9.32	advanced	96	112	110	2.75	1.85	0.64	0.73	S: 61, I: 63
15	**Prakash Kirappa Talwar**	65	male	nil	6/9(p)	6/6(p)	HTN	WNL	C:D 0.2	NIL	22.4	24	OD: OPEN, OS: OPEN	30-2 SITA STD	-1.73db	3.46	early	112	143	145	2.8	0.18	0.07	2.62	S: 67, I: 66
16	**Anwar Husain Mohammad**	53	male	present	6/6(p)	6/6	nil	WNL	C:D 0.4	OS: thinning of NRR, pallor +, nasalisation, bayonetting, laminar dot	15.3	12	OD: OPEN, OS: OPEN	30-2 SITA STD	-3.24db	2.25	early	85	101	98	3.16	1.39	0.44	1.76	S: 68, I: 70
17	**Valentione Britto**	60	male	nil	6/9	6/6	DM, HTN	WNL	C:D 0.3	NIL	24.8	22	OD: OPEN, OS: OPEN	30-2 SITA STD	-4.68db	3.54	early	105	124	141	2.32	0.69	0.3	1.63	S: 73, I: 67
18	**Shrikrishna Mahadevappa Vanahalli**	66	male	nil	6/36	6/12	DM	WNL	C:D 0.3	NIL	22.4	24	OD: OPEN, OS: OPEN	30-2 SITA STD	-2.87db	4.52	early	99	130	117	2.35	1.13	0.48	1.22	S: 66, I: 61
19	**Irappa Gadekar**	65	male	nil	6/24	6/6(p)	nil	WNL	C:D 0.9	OU: Thinning +, PPA+	18.6	16	OD: OPEN, OS: OPEN	30-2 SITA STD	-8.85db	6.5	moderate	65	68	84	3.1	2.45	0.79	0.65	S: 54, I: 52
20	**Ramdas Sanu Rane**	62	male	nil	6/18	6/6(p)	HTN	WNL	C:D 0.5	OU: nasalisation of vessels, thinning of NRR, notching+, PPA+	27.7	24	OD: OPEN, OS: OPEN	30-2 SITA STD	-21.93db	6.73	advanced	94	117	127	2.69	1.73	0.64	0.84	S: 51, I: 54
21	**Shrikant Bhairu Shinde**	67	male	nil	6/12(p)	6/6(p)	HTN	WNL	C:D 0.7	NIL	14.6	14	OD: OPEN, OS: OPEN	30-2 SITA STD	-2.91db	6.63	early	93	117	127	2.69	1.73	0.64	0.97	S: 60,I: 62
22	**Basayya Shivamorthayya Hiremath**	70	male	present	6/18	6/9(p)	DM	WNL	C:D 0.5	OU: thinning of NRR	13.5	14	OD: OPEN, OS: OPEN	30-2 SITA STD	-0.83db	2.04	early	101	93	147	2.7	0.86	0.32	1.84	S: 40, I: 75
23	**Deepak Anthony Pillay**	53	male	nil	6/6	6/6	nil	WNL	C:D 0.7	OU: thinning of NRR, laminar dot, PPA+, OS: bayonetting, notching +	18.6	9	OD: OPEN, OS: OPEN	30-2 SITA STD	-18.50db	9.34	advanced	72	87	93	2.15	1.8	0.84	0.35	S: 40, I: 72
24	**Yogesh Pandurang Chitnis**	48	male	nil	6/6	6/6	DM	WNL	C:D 0.5	OU: nasalisation of vessels	18.4	20	OD: OPEN, OS: OPEN	30-2 SITA STD	-1.79db	1.38	early	108	129	131	3.73	2.59	0.69	1.14	S: 73, I: 74
25	**Arun Vasudev Khadekar**	65	male	nil	6/12(p)	6/6	DM	WNL	C:D 0.7	OU: thinning of NRR, laminar dot, PPA+, notching +	47.5	42	OD: OPEN, OS: OPEN	30-2 SITA STD	-19.30db	11.1	advanced	43	42	39	3.06	2.68	0.88	0.37	S: 32, I: 30

26	**Shaukhat Rajesab Halakarni**	54	male	present	6/36	6/12	nil	grade I RAPD +	C:D 0.8	OD: optic atrophy+, laminar dot, bayonetting, notching, nasalisation of vessels +, OD: thinning of NRR	41.1	38	OD: OPEN, OS: OPEN	30-2 SITA STD	-23.45db	12.9	advanced	77	87	105	1.96	1.45	0.89	0.52	S: 28, I: 38
27	**Indrawwa Hanamant Bagay**	47	female	nil	6/36	6/12	HTN	WNL	C:D 0.6	OD: splinter hemorrhages +, OS: inferior thinning +	22.3	24	OD: OPEN, OS: OPEN	30-2 SITA STD	-4.04db	4.44	early	102	137	116	3.17	2.22	0.7	0.95	S: 78, I: 75
28	**Basalingappa Basappa Hasamani**	80	male	present	6/24(p)	6/12	HTN	WNL	C:D 0.6	OS: pallor +nt	32.5	26	OD: OPEN, OS: OPEN	30-2 SITA STD	-11.31db	9.16	moderate	63	71	62	3.05	1.85	0.61	1.2	S: 56, I: 50
29	**Irappa Banishetti**	59	male	nil	6/12	6/9	nil	WNL	C:D 0.3	OD: WNL, OS: NRR thinning present	10.6	12	OD: OPEN, OS: OPEN	30-2 SITA STD	-10.49db	7.78	moderate	82	105	107	2.85	0.54	0.19	2.31	S:84, I: 79
30	**Gurusidda Bhimappa Sangate**	54	male	nil	6/9	6/6	DM	WNL	C:D 0.7	OD: disc pallor +, OS: presence of notching superiorly	11.8	18	OD: OPEN, OS: OPEN	30-2 SITA STD	-1.17 db	1.89	early	94	117	120	2.42	1.39	0.57	1.03	S: 72, I: 67
31	**Reshma Kutuboddin Kazi**	37	female	nil	6/18(p)	6/9	Thyroid	WNL	C:D 0.5	OD, OS: mild thinning present	21.7	24	OD: OPEN, OS: OPEN	30-2 SITA STD	-6.86db	5.68	early	115	137	142	2.83	1.45	0.51	1.38	S: 79, I: 84
32	**Champavva Mallgouda Kurli**	71	female	nil	6/18(p)	6/9(p)	HTN	WNL	C:D 0.8	OD: pallor+, bayonetting+, PPA+, OS: pallor +, nasalisation of vessels+, laminar dot sign and bayonetting +	29.2	34	OD: OPEN, OS: OPEN	30-2 SITA STD	21.96db	8.89	severe	47	56	24	2.39	1.77	0.74	0.62	S: 42, I: 39
33	**Mallappa Dundappa Kankanewali**	73	male	present	6/9(p)	6/6	CKD	WNL	C:D 0.9	OD: cupping+, OS: PPA+	28.6	28	OD: OPEN, OS: OPEN	30-2 SITA STD	-6.40db	4.77	moderate	58	55	71	2.9	2.05	0.71	0.85	S: 51, I: 52
34	**Narayan Anantrao Joshi**	73	male	nil	6/18	6/9(p)	DM, HTN	WNL	C:D 0.7-0.8	OD: thinning+, OS: thinning +, nasalisation of vessels +	27.2	28	OD: OPEN, OS: OPEN	30-2 SITA STD	-12.31db	9.72	severe	58	74	72	3.25	2.84	0.87	0.42	S: 69, I: 76